 doi:10.20944/preprints202011.0262.v1

Review

Composites, Fabrication and Application of Polyvinylidene Fluoride for Flexible Electromechanical Devices: A Review

Shuaibing Guo [1], Xuexin Duan [1], Mengying Xie [1], Kean Chin Aw [2] and Qiannan Xue [1,*]

[1] State Key Laboratory of Precision Measuring Technology & Instruments, College of Precision Instrument and Opto-electronics Engineering, Tianjin University, China
[2] Department Mechanical Engineering, University of Auckland, New Zealand
* Correspondence: qiannanxue@tju.edu.cn

Abstract: The technological development of piezoelectric materials is crucial for developing wearable and flexible electromechanical devices. There are many inorganic materials with piezoelectric effects, such as piezoelectric ceramics, aluminum nitride, and zinc oxide. They all have very high piezoelectric coefficients and large piezoelectric response ranges. The characteristics of high hardness and low tenacity make inorganic piezoelectric materials unsuitable for flexible devices that require frequent bending. Polyvinylidene fluoride (PVDF) and its derivatives are the most popular materials used in flexible electromechanical devices in recent years and have high flexibility, high sensitivity, high ductility, and a certain piezoelectric coefficient. Owing to increasing the piezoelectric coefficient of PVDF, researchers are committed to optimizing PVDF materials and enhancing their polarity by a series of means to further improve their mechanical–electrical conversion efficiency. This paper reviews the latest PVDF-related optimization materials, related processing and polarization methods, and the applications of these materials such as those in wearable functional devices, chemical sensors, biosensors, and flexible actuator devices for flexible micro-electromechanical devices. We also discuss the challenges of wearable devices based on flexible piezoelectric polymer, consider where further practical applications could be.

Keywords: PVDF; piezoelectric polymer; wearable device; flexible sensor; electromechanical.

1. Introduction

Piezoelectric materials have been in development for 140 years[1]. These materials are widely used in electromechanical devices because they can convert mechanical energy to electrical energy under pressure or generate mechanical motion by electricity[2,3]. The use of piezoelectric materials for the preparation of micro-electromechanical devices makes it possible to develop miniature resonators[4-8], frequency meters[9] and micro energy supply chips[10-14]. Piezoelectric crystals have a single crystal structure and natural piezoelectricity, such as α-quartz[15,16]. In addition to natural piezoelectric materials that can adapt to different application scenarios, researchers have also manufactured many high-performance artificial piezoelectric materials. Typical piezoelectric-crystal materials include aluminum nitride (AlN) and zinc oxide (ZnO)[17,18], which have a variety of advantages, such as very high strength, large piezoelectric coefficients, and good applicability to micro devices[19,20]. Piezoelectric ceramics consist of many small crystals and the crystals are randomly oriented. The crystal orientation can be changed through a polarization process to exhibit piezoelectricity. The polarization process is usually performed by applying a high electric field. PZT-series materials such as PMN-PZT and PMMPT are typical representatives of piezoelectric ceramics; they not only have high piezoelectric coefficients but also good ductilities. However, the bending property of PZT-series materials is still poor, and they pollute the environment because of their lead content. Generally, these inorganic piezoelectric materials have the features of high hardness and brittleness, which are not suitable for flexible devices that require high material flexibility.

With the rapid development of wearable devices, there is an increasing demand for device flexibility. Compared with inorganic and ceramic materials, piezoelectric polymers have more remarkable bending and tensile properties. Polymer piezoelectric materials have a carbon chain as the backbone, and their flexibility is higher than those of single crystals and ceramics[21-23]. This high flexibility allows them to withstand a greater amount of strain, thus making them more suitable for application scenarios with large bending and twisting requirements. Some suitable piezoelectric polymers, such as polyvinylidene fluoride (PVDF), polyvinylidene fluoride-trifluoro ethylene (P(VDF-TrFE)), cellulose and its derivatives, polyamides, and polylactic acids, are widely used in ultrasonic sensors, audio sensors, medical sensors, display equipment, vibrometers, impact sensors, pressure sensors, and many other applications[24]. Among flexible piezoelectric materials, PVDF has a high piezoelectric coefficient, good flexibility, and excellent biocompatibility; therefore, PVDF is widely used to develop flexible electromechanical devices.

However, improvement of the polarization characteristics of flexible piezoelectric materials continues to be challenging. The piezoelectric coefficient of PVDF can be effectively improved by doping with inorganic piezoelectric materials, such as PZT and piezoelectric ceramics. In addition, nano-clay, BTO, Ag, graphene, and other nanomaterials can change the crystal structure of PVDF and increase the β phase proportion. Moreover, some new fabrication methods can also improve the polarity of flexible piezoelectric materials. In this paper, the recent progress in material science of PVDF and PVDF composites, aiming for micro fabrication techniques, is reviewed. We discuss the latest technological scheme and processing methods and compare their merits and demerits. The improvement in the performance of flexible piezoelectric materials has overcome the limitations of wearable electromechanical devices. The applications of these materials in electromechanical devices are discussed in detail. Finally, the development trend of flexible electromechanical devices based on PVDF is prospected in the future, such as using the help of piezoelectric properties of biocrystals, improving the biocompatibility and for the development of bionic devices.

2. Polyvinylidene fluoride-based-series piezoelectric material

2.1. The piezoelectric effect principle of PVDF

The piezoelectric effect[25,26] refers to the polarization of certain dielectrics in a specific direction under the action of an external force. A dielectric material has positive and negative charges on two opposite surfaces. When the external force is eliminated, the material returns to a neutral state. This phenomenon is called the positive piezoelectric effect. As the direction of the force changes, the polarity of the charge also changes. Conversely, when an electric field is applied in the polarization direction of the dielectric, the material will deform. When the electric field is removed, the deformation disappears. This phenomenon is called the reverse piezoelectric effect. The fundamental reason for the piezoelectric effect is that the mechanical deformation caused by the polarization intensity is linear with respect to the electric field strength in crystal materials without a symmetry center.

Piezoelectric materials have unique mechanical and electrical coupling characteristics, including the direct piezoelectric effect of charge generated under the action of external mechanical stress and the reverse piezoelectric effect of mechanical strain caused by an external electric field. The direct and converse piezoelectric effects obey several equations[27-31] such as eq. (1).

$$\begin{bmatrix}\delta\\ D\end{bmatrix} = \begin{bmatrix}s^e & d^t\\ d & \varepsilon^T\end{bmatrix}\begin{bmatrix}\sigma\\ E\end{bmatrix}, \tag{1}$$

where δ and D represent the strain component and electric displacement component, respectively; s and e represent the elastic compliance and constant under a constant electric field, respectively; d represents the piezoelectric coefficient; t represents the transposition; ε and T represent the dielectric constant and constant stress, respectively; σ and E represent the stress and electric field components, respectively. The direct piezoelectric effect is very important for the sensing and energy collection of surface charge generated by applied stress on piezoelectric materials.

Preprints (www.preprints.org) | NOT PEER-REVIEWED | Posted: 9 November 2020 doi:10.20944/preprints202011.0262.v1

Many piezoelectric materials have a very clear polar axis. Energy harvesting performance is related to the angle between the stress and polar axis. The direction of the polar axis is "3" directions, and the direction perpendicular to the polar axis is "1" direction. The direction of stress application can be along either direction "1" or "3" directions, thus forming 31-mode and 33-mode[32].

The piezoelectric properties of PVDF are directly related to its structure[33]. PVDF is a semi-crystalline polymer polymerized by H_2C =CF_2 monomer, whose properties depend on the phase due to the alignment of crystals (Figure 1a). When two CF_2 or CH_2 groups are connected, a defect occurs in the connected polymer chain. Defects in the polymeric chain influence the polarity of the PVDF film, thereby increasing the piezoelectric response. The polymer has α, β, γ, δ, and ε phases, which are five semi-crystalline polymorphs. The α and β phases are the most common phases. The γ phase, which is not common, is a transitional state between α and β. δ and ε are difficult to isolate. The α phase of PVDF is non-polar[34], because it contains two molecular chains and the dipole moments are reversed, forming a trans-gauche conformation (TGTG') (Figure 1b). The β phase of PVDF has an all-trans conformation (TTTT) (Figure 1c). Most hydrogen atoms and fluorine atoms are separated; therefore, it has a dipole moment perpendicular to the polymer chain, which shows the highest net dipole moment. The γ phase of PVDF is a transitional state between α and β (Figure 1d), it has a smaller dipole moment than the β phase[35]. It is necessary to increase the proportion of β phase in PVDF to maximize its electromechanical conversion efficiency[36].

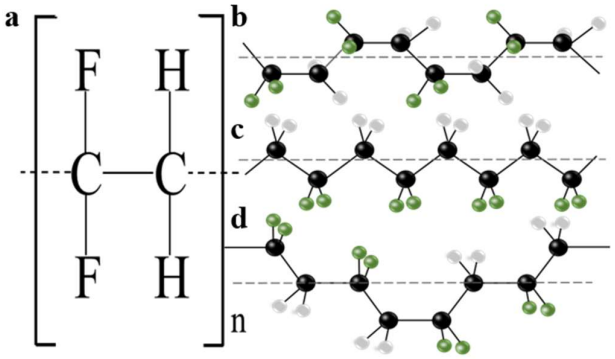

Figure 1. (a) Structure of PVDF; **(b)** Space structure of α-phase PVDF; **(c)** Space structure of β-phase PVDF; **(d)** Space structure of γ-phase PVDF.

2.2. Piezoelectric materials based on PVDF and its derivatives

Polymer piezoelectric material is a material with a carbon chain as the basic skeleton, and its flexibility is higher than that of single crystals and ceramics[21,22]. This high flexibility allows it to withstand a greater amount of strain, thereby making it more suitable for application scenarios with large bending and twisting requirements. Some good piezoelectric polymers such as PVDF, polyvinylidene fluoride-trifluoro ethylene (P(VDF-TrFE)) (Figure 2a), cellulose and its derivatives, polyamides, and polylactic acids are widely used in ultrasonic sensors, audio sensors, medical sensors, display equipment, vibrometers, impact sensors, pressure sensors, and many other applications[24].

Piezoelectric polymer PVDF and its copolymers have the advantages of natural flexibility, easy processing, and sufficient mechanical strength, which make them more suitable for flexible sensors than inorganic piezoelectric materials[37-43].

So far, PVDF has been found to exist as five semi-crystalline polymorphs: α, β, γ, δ, and ε. Among these, α-phase (TGTG0 conformation) is not electroactive, and β-phase has the strongest piezoelectricity. PVDF with a low component of β-phase has a d_{33} value of approximately 20-30 pC/N[44-51]. Therefore, increasing the β-phase PVDF composition is vital to enlarge the mechanical–electrical energy conversion performance of PVDF. Therefore, the piezoelectric coefficient of PVDF is lower than that of common inorganic piezoelectric materials. Chang et al.[43] prepared PVDF nanofibers with a high β-phase PVDF component by near-field electrospinning (Figure 2a). The fiber-based generator could provide a maximum output power with 5–30 mV and 0.5–3 nA voltage and

 doi:10.20944/preprints202011.0262.v1

current, respectively (Figure 2c). It has a much higher energy conversion efficiency than generators made of PVDF thin films[43].

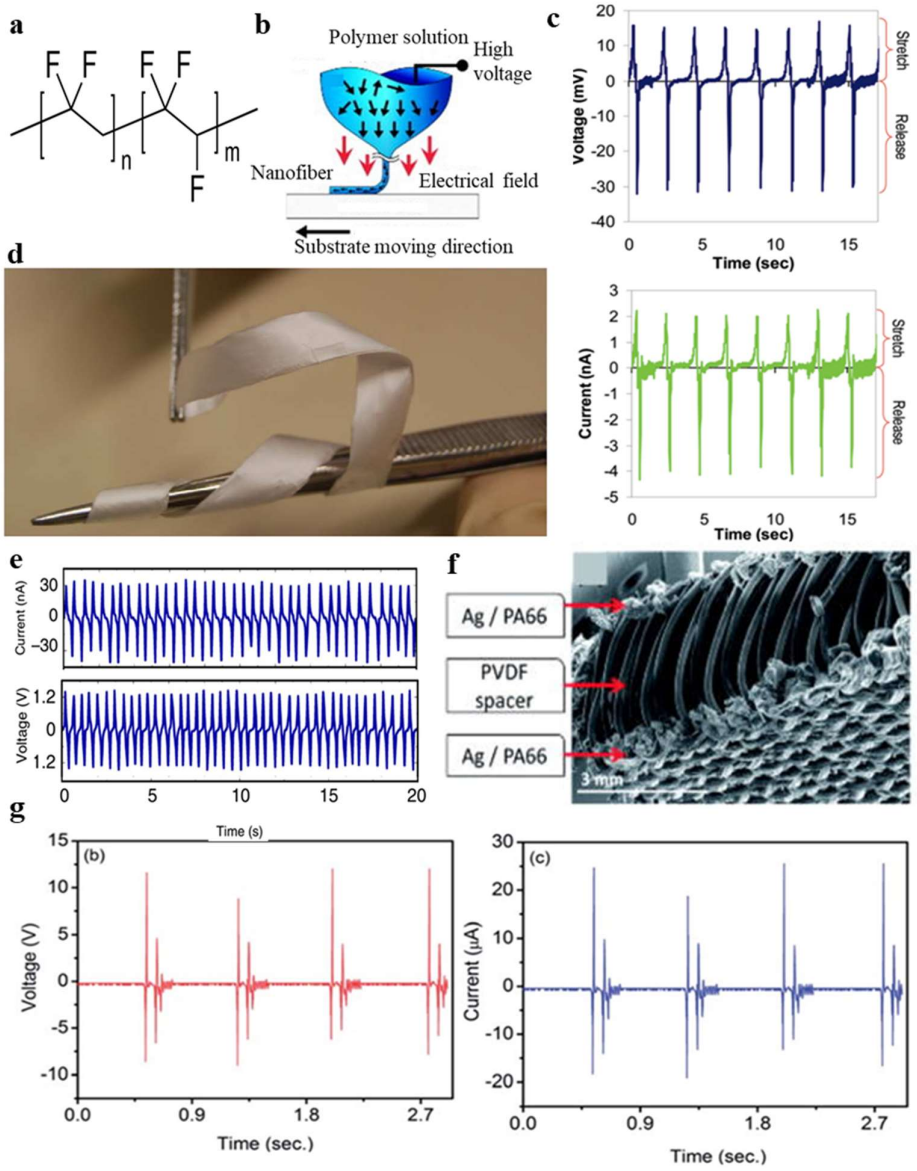

Figure 2. (a) Structure of P(VDF-TrFE) [41]; **(b)** PVDF nanofibers with the high component of β-phase PVDF by near-field electrospinning[43]; **(c)** The generator based on fiber could provide a maximum output power is 5-30 mV and 0.5-3 nA with different feature sizes[43]; **(d)** A free-standing film's photograph and SEM image [44]; **(e)** The output power of the generators based on textile[44]; **(f)** The "3D spacer" cross-sectional SEM image[52]; **(g)** 2D and 3D piezoelectric textile's output power[52].

The P(VDF-TrFE) copolymer has high crystallinity and piezoelectric properties, so it has a high piezoelectric response[53-55]. Persano et al.[44] proposed a piezoelectric textile based on highly aligned electrospun P(VDF-TrFE) fibers. The proposed piezoelectric textile has a large area, and it is flexible and freestanding (Figure 2d)[44]. The maximum open-circuit voltage of the generators based on textiles can reach 1.5 V (Figure 2e)[44], thus showing excellent flexibility and mechanical strength. Many new designs have emerged in the practice field to produce all-fiber piezoelectric textiles. A "3D spacer" based on all-fiber piezoelectric textiles was reported[52], consisting of top and bottom electrodes and a spacer yarn. The spacer yarn is composed of high concentration of β-phase PVDF monofilaments. The top and bottom electrodes are composed of silver-coated polyamide

Preprints (www.preprints.org) | NOT PEER-REVIEWED | Posted: 9 November 2020 doi:10.20944/preprints202011.0262.v1

multifilament yarn layers (Figure 2f)[52]. The new type of 3D textile-based PVDF generator had a much larger output power density than the traditional 2D piezoelectric textile, up to 5.07 lW/cm^2 [56-60] (Figure 2g)[52].

2.3. Piezoelectric materials doped in PVDF

To balance the contradiction between flexibility and higher voltage coefficient, researchers have tried to mix polymer piezoelectric materials with inorganic piezoelectric materials. Because of the good piezoelectric properties and relatively soft properties of PZT and the tensile and flexural properties of PVDF, the combination of the two will make sense. According to the above ideas, Tiwari et al.[61] prepared PZT and PVDF piezoelectric composite films using solution casting technology. This method can achieve both electric field polarization and mechanical stretching during the electrospinning process, making it very suitable for manufacturing piezoelectric nanofibers. Similarly, the dielectric properties of PZT/P (VDF-TrFE) composite films[62] were also studied. In 2020, Pal et al.[63] used lanthanum-doped lead zirconate titanate (PLZT), PVDF, and multi-walled carbon nanotubes (MWCNTs) as supplementary fillers to create a three-phase hybrid piezoelectric nanogenerator. Figure 3a shows the variation of stored power with time and SEM of PLZT particles dispersed in the PVDF matrix. Raad et al.[64] fabricated nanogenerator devices on the basis of composite structure of PVDF, ZnO, nanorods, and $BaTiO_3$. The voltage output of these composite structures are up to 12 V under the force of 1.5 N (Figure 3b).

Considering the compatibility with the human body, lead-free materials are more popular. Titanate or bismuth[65] are mixed with PVDF to develop lead-free piezoelectric nanofiber composites. The piezoelectric properties of PVDF can be changed by adding calcined $BaTiO_3$ ceramic powder[66,67].

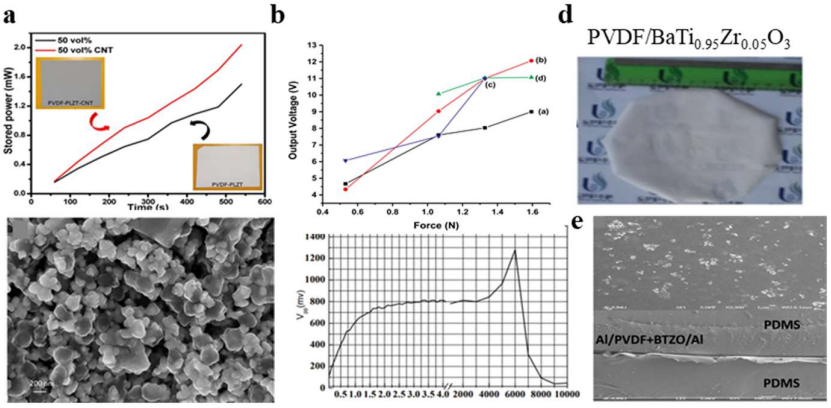

Figure 3. (a) Variation of stored power with time and SEM of PLZT particles dispersed in the PVDF matrix[63]; **(b)** The relationship between output voltage and applied forces with different frequencies[64]; **(c)** Relationship between output frequency and voltage of PVDF nanofiber composite containing BNT-ST[9]; **(d)** Optical diagram PVDF/BTZO hybrid film[68]; **(e)** SEM of PVDF/BTZO hybrid film[68].

Researchers at Kyungnam University have synthesized an excellent lead-free piezoelectric material[9], which is a kind of flexible lead-free piezoelectric nanofiber composite of BNT-ST((1-x)$Bi_{0.5}Na_{0.5}TiO_3$- xSrTiO) ceramics and PVDF polymer,

which were fabricated by electrospinning. By measuring the functional relationship between the output frequency and voltage of the PVDF nanofiber composite containing BNT-ST (Figure 3c)[9], the piezoelectric properties of the composite and the sensitivity of the piezoelectric output to frequency are substantially improved. This is because BNT-series materials can overcome large coercive field defects and exhibit strong piezoelectric properties[69-73].

In 2015, Alluri et al.[68] developed a flexible hybrid film of PVDF doped with highly crystalline $BaTi_{(1-x)}ZrxO_3$ (x = 0, 0.05, 0.1, 0.15, and 0.2) nanocomposites (BTZO). During preparation, the PVDF matrix solution was embedded in BTZO using a molten-salt process under ultrasonication (Figure 3d)[68]. The SEM images of the PVDF/BTZO hybrid film are shown in Figure 3e. It can be concluded that by the molten salt method, replacing the Ti4+ (0.605 Å) site with a Zr4+ atom (0.72 Å) can modify the high-purity bulk $BaTiO_3$

Preprints (www.preprints.org) | NOT PEER-REVIEWED | Posted: 9 November 2020 doi:10.20944/preprints202011.0262.v1

nanocomposites and enhance the piezoelectric coefficient (d_{33}) from 100 pC/N ($BaTiO_3$)[74-78] to 174-236 pC/N ($BaTi_{(1-x)}Zr_xO_3$)[79-83]. The properties of BTZO/PVDF hybrid films have been substantially improved compared to those of pure piezoelectric films and have great potential in manufacturing environmental protection devices, active sensors, and flexible nanogenerators.

2.4. Conductive nanomaterials doped in PVDF

Although polymer materials have the advantages of high flexibility and high mechanical strength compared to inorganic materials, the piezoelectric coefficient of piezoelectric materials is relatively small; moreover, their piezoelectric conversion efficiency is low, and they do not easily conduct electricity. The introduction of nanomaterials may change the crystal structure of polymer piezoelectric polymers and improve the piezoelectric properties[84-89]. Zirconate titanate, barium titanate, and zinc oxide have high piezoelectric constants; therefore, polymer piezoelectric matrices usually use them as piezoelectric fillers[90-95]. Compared with those of the pure piezoelectric polymer, the piezoelectric properties of the nanocomposites are improved, dielectric constant is significantly increased, crystallinity of the phase is increased, and local stress is increased. Adding nanoclay[96] to PVDF can prompt the formation of the β-phase in the spinning process, which is an ideal method to prepare piezoelectric nanofibers. BTO nanoparticles were used to improve the P(VDF-TrFE) nanofibers' piezoelectric sensing properties (Figure 4a)[97]. BTO/P(VDF-TrFE) nanofibers doped with BTO nanoparticles have the largest β-phase crystallinity and the best piezoelectric properties.

Wu et al.[98] studied the piezoelectric properties, crystal structure, and sound absorption properties of PVDF nanofibers doped with carbon nanotubes prepared by electrospinning.. The results show that adding CNTs further improves the piezoelectric properties and the ability to absorb sound waves at low frequencies. Hosseini et al.[99] studied the potential synergistic effect of OMMT and MWCNT nanofillers on PVDF crystal structure and piezoelectric device performance. They evaluated PVDF fiber mats' sound-absorbing and piezoelectric properties, and the results showed that compared with OMMT, the MWCNT could decrease PVDF impedance and increase the dielectric constant. MWCNT/OMMT hybrid nanocomposites have good sound absorption properties, which might be caused by the enhanced interaction at the polymer-filled interface between the acoustic wave and OMMT plates and MWCNT nanotubes[100-104]. They found that the sound absorption efficiency of PVDF/MWCNT/OMMT hybrid nanocomposites was higher than that of pure PVDF fibers and film. Negar et al.[11] fabricated PVDF nanocomposites by doping with PZT particles. The PVDF-PZT nanocomposite fiber, the crystallization mechanism, and β-phase formation based on the addition of PZT are shown in Figure 4b.

PVDF and graphene-silver (GAg) nanocomposites have plasma-coupled piezoelectric properties, and the piezoelectric energy conversion efficiency reaches 15%[105]. Using the unique interface structure of silver nanoparticles, silver-doped oriented PVDF nanofibers with a high content of β phase were prepared by electrospinning[106], and the crystallinity of the β phase was 44.5%. Silver nanoparticles in graphene dispersion form n-type doping on graphene owing to electrostatic effects [107-111]. The self-polarization of silver nanoparticles in PVDF is beneficial to the nucleation of the electroactive β phase. PVDF nanocomposites are environmentally friendly and low-cost nanocomposites, having high piezoelectric coefficients and different piezoelectric coefficients under different light conditions (Figure 4c)[105].

Gan et al.[112] developed composite materials using TiO_2 nanoparticles and PVDF. The increase in conductivity makes the polarization process easier, and the required electric field is smaller (260-120 mV/m). In 2017, Al-Saygh et al.[113] proposed a flexible pressure sensor based on PVDF doped with rGO and TiO_2 nanolayers (TNL). The hybrid PVF/rGO-TNL film had a higher β-phase content (75.68%) than PVDF (70.37%), PVDF/rGO (72.73%), and PVDF/TNL (73.5%) films. Similarly, Pusty et al.[114] combined iron with carbon nanotubes and graphene nanomaterials and proposed that adding CNT and Fe-RGO to PVDF can increase the conductivity of nanocomposite membranes. Mishra et al.[115] developed a flexible piezoelectric polymer nanocomposite film to collect mechanical energy, which is based on PVDF doped with gallium ferrite nanoparticles (GFO). Under mechanical pressure and release conditions, the output voltage and current are 3.5 V and 4 nA, respectively (Figure 4d)). As a type of piezoelectric ceramic, nano ZnO is also used as a piezoelectric filler[116]. Dodds et al.[117] prepared PVDF TrFE/ZnO nanoparticle films by spin coating and studied their piezoelectric response. The prepared films not only maintain their mechanical flexibility but also improve their piezoelectric properties. Zinc oxide-PVDF composite membrane[118] can also be prepared by sol-gel technology. The latest report is on the preparation of metal ZnO PVDF composite films by doping ZnO

Preprints (www.preprints.org) | NOT PEER-REVIEWED | Posted: 9 November 2020 doi:10.20944/preprints202011.0262.v1

nanoparticles into metals, which shows the potential for mechanical energy generation and motion sensing. Figure 4e shows the fabrication process of the device. They respectively studied and compared the voltage output of pure ZnO-PVDF samples and ZnO-PVDF composites doped with sodium (Na), cobalt (Co), silver (Ag), ferric oxide (Fe_3O_4), and lithium (Li)[119].

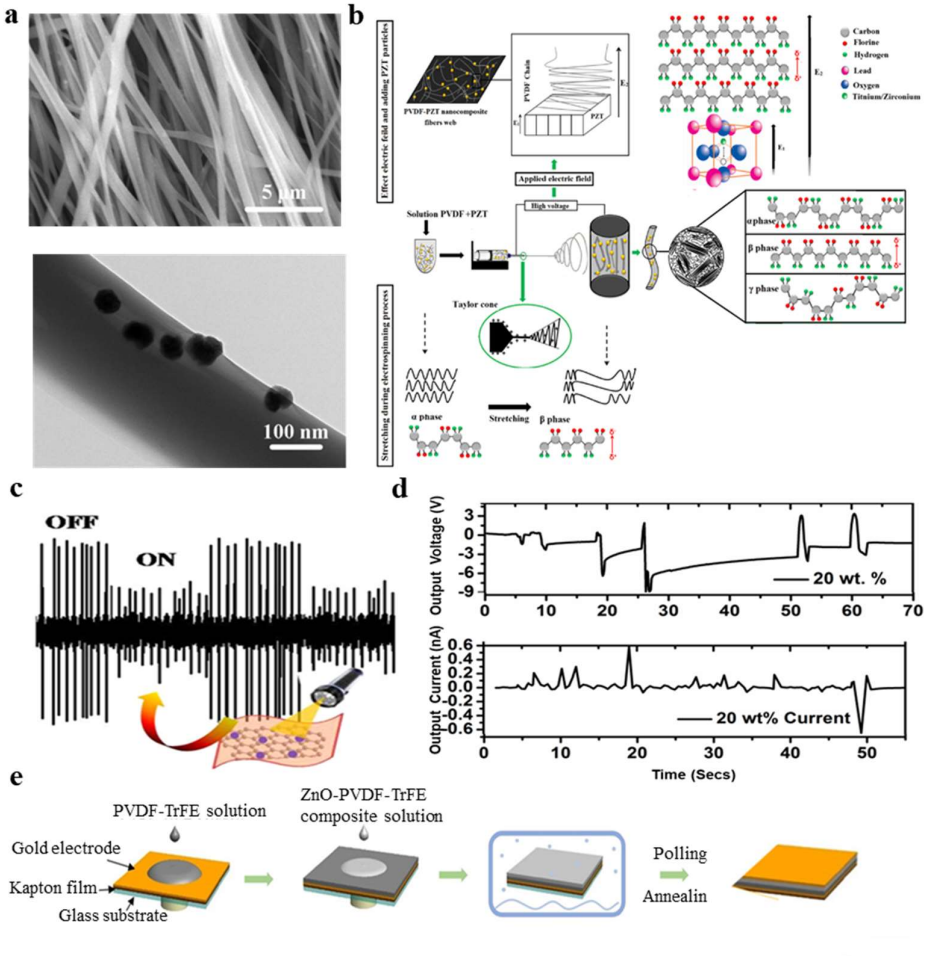

Figure 4. (a) The SEM of BTO/P(VDF-TrFE) nanocomposite fiber[97]; **(b)** PVDF-PZT nanocomposite fiber, the crystallization mechanism, and β-phase formation based on adding PZT[11]; **(c)** Change of piezoelectric coefficient in the form of output voltage under different light conditions[105]; **(d)** Output voltage and current signal of GFO-PVDF composite films[115]; **(e)** Schematic of the manufacturing process of the device[119].

2.5. Biomaterials functional PVDF

Some biomaterials have certain piezoelectric properties naturally. In 2017, Nuraeva et al.[120] investigated (S)-glutamine and ortho-carboranyl derivatives of (S)-asparagine films and bulk crystal piezoelectric properties, demonstrating a very high piezoelectric response. The high local transverse piezoelectric coefficients of these biocrystals indicate that they are promising materials for various piezoelectric applications. Stapleton et al.[121] provided experimental evidence of the globulin and lysozyme's direct piezoelectric effect. They measured the direct piezoelectric effect of the lysozyme crystal aggregation film and found that the average piezoelectric coefficients of the monoclinic and tetragonal lysozyme films were 0.94 pC/N and 3.16 pC/N, respectively (Figure 5a). Nguyen et al.[122] reported that diphenylalanine (FF) is a short peptide composed of two natural amino acids, with special piezoelectric properties and excellent mechanical properties(Figure 5b). Doping with a piezoelectric polymer can stimulate the piezoelectric properties. Recently, Yang et al.[123] modified barium titanate (BTO) with polydopamine (PDA). Then, the mixing ratio was adjusted between it and the PVDF matrix, and finally formed a uniform and homogeneous PDA @ BTO / PVDF composite material. The facial solution-

Preprints (www.preprints.org) | NOT PEER-REVIEWED | Posted: 9 November 2020 doi:10.20944/preprints202011.0262.v1

casting method was used to make the flexible piezoelectric pressure sensor shown in Figure 5c. PDA can improve the dispersion of BTO in the PVDF matrix, reduce interface void defects and cracks between the two components. The output voltage is about 2 times higher than the unmodified one, and 13.3 times higher than the original PVDF. Tamang et al.[124] reported that DNA was used as a nucleating agent to produce a self-polarized PVDF membrane with higher piezoelectric properties (Figure 5d). This nucleating agent can achieve the molecular dipole arrangement and the nucleation of the electroactive β phase in PVDF. Phosphate ions interact with hydrogen bonds on the single-strand deoxyribonucleic acid (ss-DNA) backbone to form a stable polar β phase, accounting for more than 80% of polar β-phase in the PVDF matrix (Figure 5e).

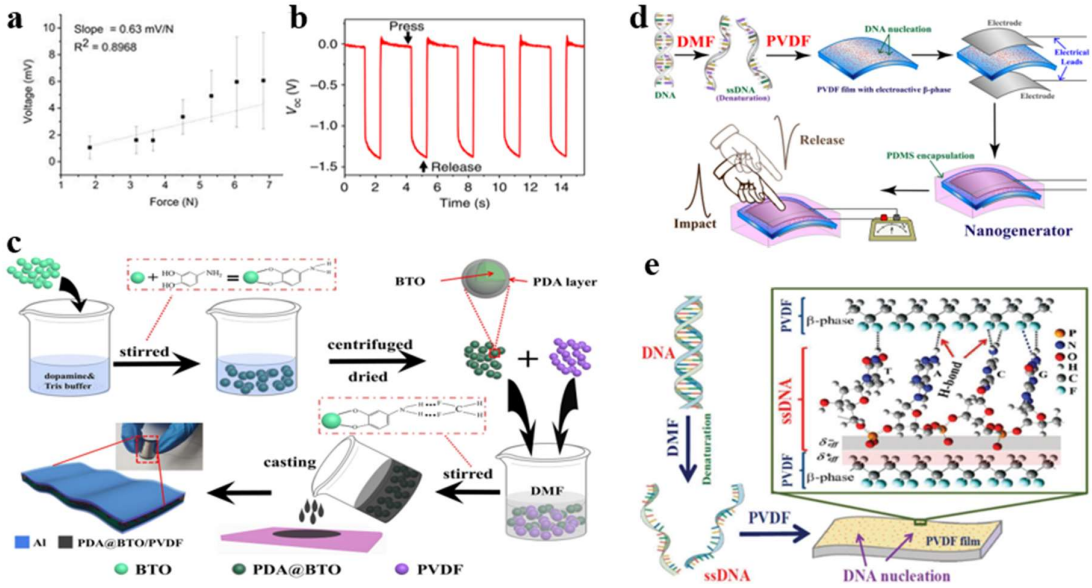

Figure 5. (a) Piezoelectric voltage generated increases with increasing applied force[121]; **(b)** Open-circuit voltage of the FF-generator[122]; **(c)** The fabrication process of PDA@BTO/PVDF composite membrane on the basis of flexible pressure sensor[123]; **(d)** DNA was used as a nucleating miagent to produce a self-polarized PVDF membrane to fabricate nanogenerator[124]; **(e)** Denaturation of DNA and the forming process of ß-enriched DNA-PVDF membrane[124].

3. Fabrication and polarization of PVDF

There are many methods to convert PVDF into the β phase, including electrospinning, spin coating, solvent casting, and 3D printing. PVDF processed by the two spin coating and solvent casting methods mainly forms the α phase; therefore, a subsequent polarization method is needed to increase the β phase state of PVDF[125,126]. Polarization can be achieved with a set of widely used techniques that can be used to reorient polymers to increase the net polarization vector in 3 directions, which is an important step during the fabrication process. For the processing methods of electrospinning and 3D printing, the polarization process can be completed directly in situ under the action of an electric field and temperature, and no subsequent polarization process is required. The following sections mainly discuss the preparation and polarization methods of PVDF films, including the piezoelectric effect principle.

3.1. Fabrication of PVDF by spin coating and solvent casting

Spin coating and solvent casting mainly form the α phase of PVDF; therefore, a subsequent polarization process is required. In the spin coating method, the surface stress is increased during the spinning process, and the addition of some compounds helps induce and contribute to the formation of the β phase state of PVDF, and sometimes it can be formed with a certain piezoelectric coefficient without subsequent polarization. A schematic diagram of the spin coating and solvent casting is shown in Figure 7a, b.

Preprints (www.preprints.org) | NOT PEER-REVIEWED | Posted: 9 November 2020 doi:10.20944/preprints202011.0262.v1

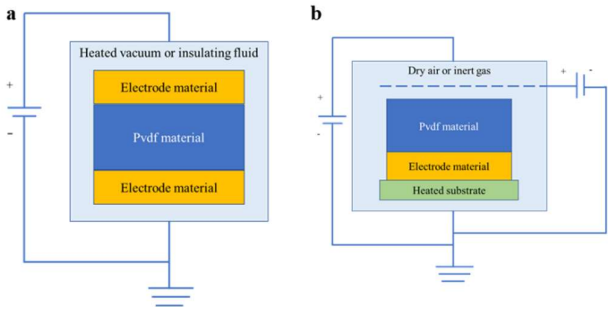

Figure 6. (a) Schematic of electrode poling method and **(b)** corona poling method.

Electrode poling and corona poling are the two most common methods of polarization. Electrode poling has the advantages of high d_{33} coefficient and reproducibility. Electrode poling is a relatively simple method among these two methods. The PVDF film is sandwiched between two electrodes and then wrapped by a shell (Figure 6a). To prevent the PVDF film from being broken down by the arc between the electrodes, the air in the shell needs to be evacuated or an insulating liquid needs to be injected into the shell[127,128]. To polarize the PVDF film, we need to apply an electric field between 5 and 100 MV/m. Corona poling needs to keep the gas in the shell dry. We can circulate dry or inert gas. The PVDF film is only in contact with one of the electrodes. The corona tip is placed on the top and connected to a 10 kV voltage. The voltage connected to the grid is much lower (10 kV), ionizing the gas between the corona tip and the grid and accelerating the movement to the PVDF film, thereby polarizing the PVDF film (Figure 6b). The electron beam poling method uses a focused electron beam and irradiates the PVDF film to reorient into the β phase. In addition to the above polarization methods, mechanical drawing and additive manufacturing can polarize PVDF. As for additive manufacturing, we can induce the formation of the β phase using composite systems. Table 1 shows the advantages of various polarization methods. The method of solvent casting mainly relies on the addition of some compounds and application of high temperature and external electric field, to promote the formation of the β phase state of PVDF. Chien et al.[129] spin-coated PVDF–TrFE dissolved in MEK and hot embossed the silicon mold on the film under DC poling (Figure 7c). The electric voltage varied from 30 to 60 V, and the temperature was 90 or 110 °C.

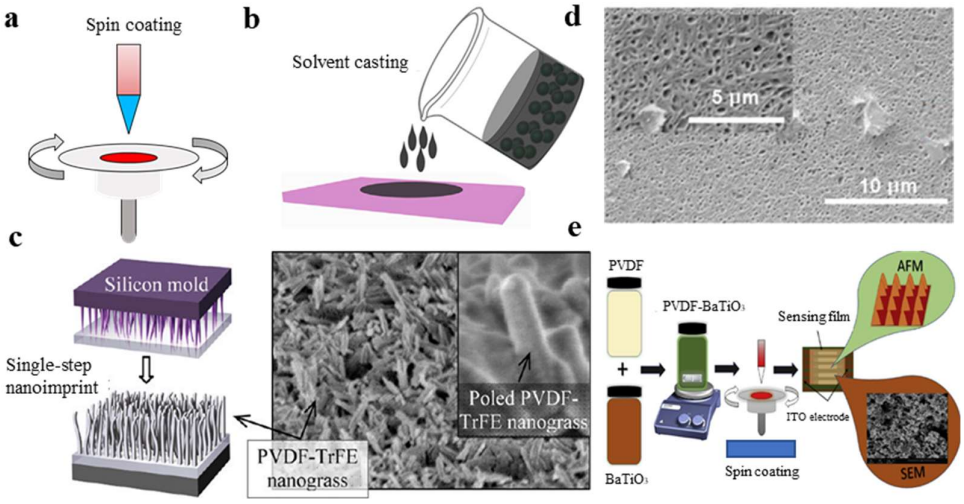

Figure 7. (a) Schematic diagram of the spin coating and **(b)** Solvent casting; **(c)** Spin coated PVDF-TrFE was dissolved in MEK and the silicon mold was hot pressed on the film [129]; **(d)** SEM of PVDF–TrFE copolymer thin films fabricated by spin coating[130]; **(e)** Preparing the PVDF-$BaTiO_3$ nanocomposite films by spin coating[131].

Preprints (www.preprints.org) | NOT PEER-REVIEWED | Posted: 9 November 2020 doi:10.20944/preprints202011.0262.v1

Table 1. The advantages of various polarization methods.

Polarization methods	Advantages
Electrode poling	High d_{33} coefficient and reproducibility
Corona poling	High d_{33} coefficient and No requirement for one end structure of the material
Additive manufacturing	Increased the design scope of the three-dimensional structure of the material and low temperature
Mechanical drawing	High d_{33} coefficient and reproducibility
Electron beam poling	Increased the design scope of the three-dimensional structure of the material

The piezoelectricity of thin films reaches as high as 14.0 pm/V, with a d_{33} value of 72.2 pC/N. Tushar et al.[130] spin-coated PVDF–TrFE copolymer into thin films to induce the formation of the β phase with a d_{33} value varying from 38 pC/N to 74 pC/N (Figure 7d). Schulze et al.[132] prepared P(VDF-TrFE) films for 20 μm thickness by solvent casting under the effect of electrode poling and an electric field of 75 MV/m. The d_{33} coefficients were measured to be about 20 pC/N. The spin-coating technique[131] was used to prepare the PVDF-$BaTiO_3$ nanocomposite films on an interdigital ITO electrode(Figure 7e). Vineet et al.[61] fabricated PVDF/PZT piezoelectric composite films by a solution cast technique. The d_{33} value varied from 60 pC/ N to 84 pC/ N. The higher the content of PZT ceramic, the greater the proportion of the β phase of PVDF.

3.2. Fabrication of PVDF by electrospinning

Electrospinning is a very promising processing technology. The needle tube containing the PVDF solution sprays the PVDF solution onto a drum through a nozzle, the substrate wraps around the drum, and a voltage between 10 and 20 kV is usually added between the nozzle and the substrate[133]. Nano- to micro-scale PVDF fibers are randomly deposited on the substrate, forming a low-density PVDF film. The electrospinning technique completes the PVDF deposition and polarization process in one step. The rotation of the drum increases the stress between PVDF and the substrate, which in turn promotes the formation of the β-phase state of PVDF. A schematic diagram of the electrospinning technique is shown in Figure 8a. Gong et al.[134] combined the PVDF nanofiber membrane by electrospinning with PDMS-Ag NWS and PET/ITO electrodes to fabricate sensors. Lu et al.[106] made a flexible bend sensor to monitor human respiration by electrospinning PVDF and a silver mixed solution (Figure 8b).

Xiaohe et al.[97] fabricated (BTO)/P(VDF-TrFE) composite nanofibers by electrospinning and were able to distinguish and sense the movement of walking ants and the energy of a free-falling ball as low as 0.6 μJ (Figure 8c). Sang et al.[9] fabricated flexible lead-free piezoelectric nanofibers composed of PVDF and BNT-ST ceramic by electrospinning. The output voltage measurement system is a frequency function for the BNT-ST/PVDF nanofiber composite module (Figure 8d). Rahul et al.[135] fabricated PVDF nanofibers with a high β phase state to develop a PVDF strain sensor to measure the string force (Figure 8e). Kunming et al.[136] fabricated nanocomposite fiber mats by electrospinning graphene nanosheets, barium titanate, and PVDF, obtaining as high as 11 V of open-circuit voltage (Figure 8f,g)).

Preprints (www.preprints.org) | NOT PEER-REVIEWED | Posted: 9 November 2020 doi:10.20944/preprints202011.0262.v1

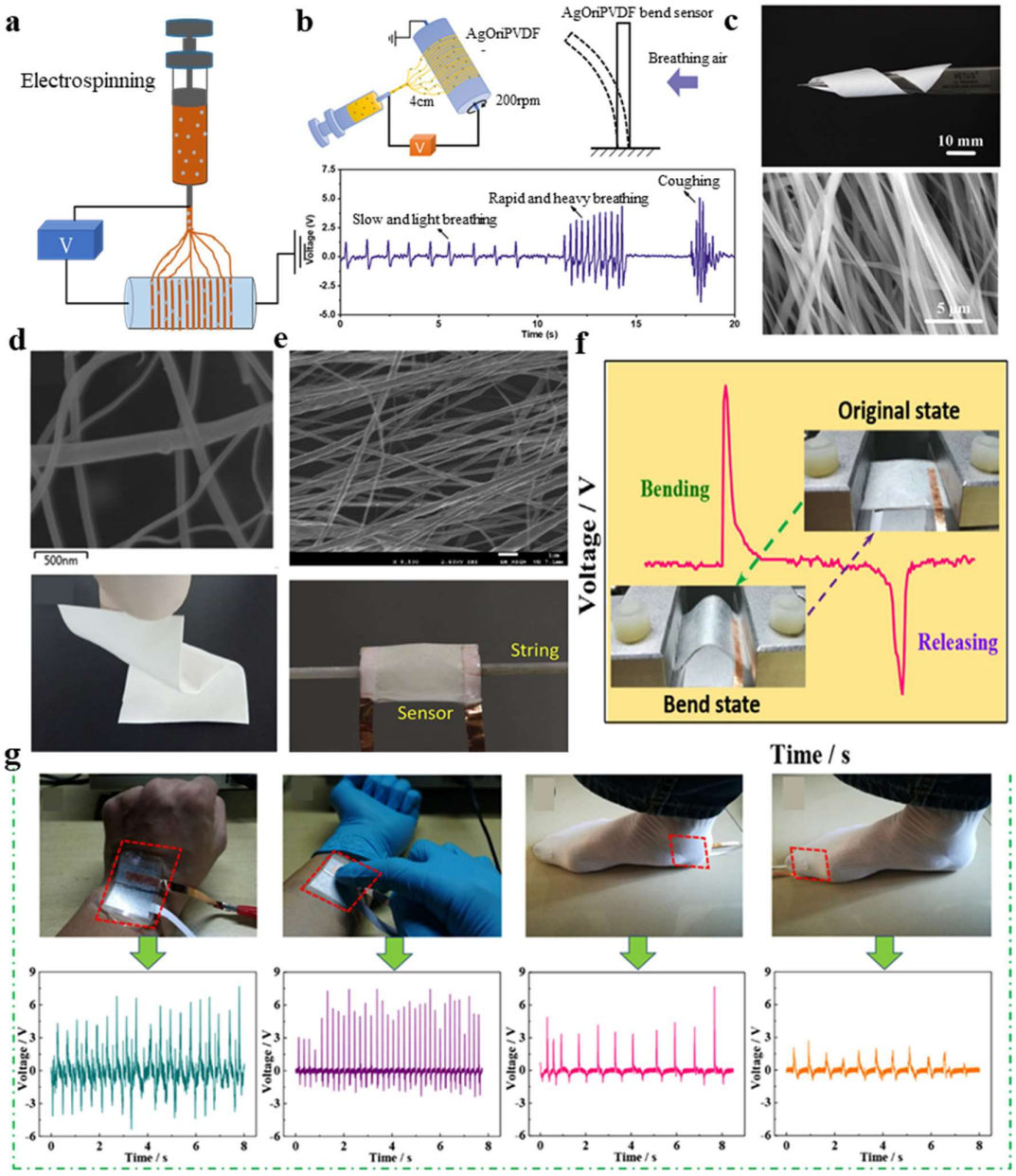

Figure 8. (a) Schematic diagram of the Electrospinning technique; **(b)** Flexible bend sensor to monitor human respiration[106]; **(c)** Optical photo and SEM of (BTO)/P(VDF-TrFE) composite nanofibers[97]; **(d)** Optical photo and SEM of BNT-ST/PVDF nanofiber composite[9]; **(e)** PVDF strain sensor for measuring the force of the string[135]; **(f)** Mechanical movement in the primitive phase and the bending phase[136]; **(g)** Optical image and output voltage generated by human movement[136].

3.3. Fabrication of PVDF devices by 3D print

The 3D print can deposit PVDF or PVDF compounds on the bottom heating plate under heating and nozzle extrusion (Figure 9a). Based on the 3D printing principles, we can incorporate polarizing processes, including heat press, electric field poling, and mechanical stretching simultaneously. The polarization process is shown in Figure 9b.

Preprints (www.preprints.org) | NOT PEER-REVIEWED | Posted: 9 November 2020 doi:10.20944/preprints202011.0262.v1

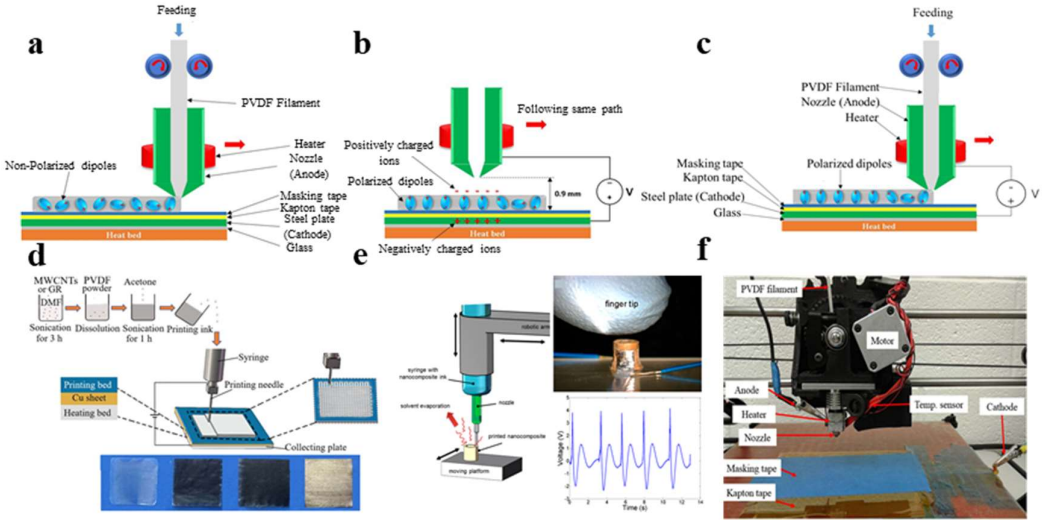

Figure 9. (a) Schematic of 3D printing of PVDF layer; **(b)** Corona poling process; **(c)** Simultaneous 3D printing and in-situ polarization; **(d)** 3D printing process and fabricated PVDF film[137]; **(e)** 3D cylindrical sensor's piezoelectric voltage output when five finger taps[138]; **(f)** Optical diagram of 3D printing technique and corona poling process[139].

Finally, we completed the integration of 3D printed PVDF and PVDF composites with the in situ polarized PVDF. The schematic is shown in Figure 9c. The shear force between the nozzle and PVDF, as well as heating, nucleation on filler surfaces, and electric field, all help to promote the formation of the β-phase state of PVDF. Hoejin et al.[140] fabricated PVDF/$BaTiO_3$ nanocomposites using a 3D printing technique. Then, the composite material was thermally polarized to improve the piezoelectric response of the composite. The piezoelectric response of the PVDF/$BaTiO_3$ nanocomposite was three times higher than that of the nanocomposites fabricated by solvent casting. Using the 3D printing technique, we can obtain a more homogeneous dispersion of PVDF/$BaTiO_3$ nanocomposites, in comparison with nanocomposites fabricated by solvent casting. Chen et al.[137] fabricated electroactive PVDF thin films of bi-axially oriented using layer-by-layer 3D printing. Carbon nanotubes were added as a nucleating agent to induce the formation of the β-phase state of PVDF (Figure 9d).

Sampada et al.[138] fabricated flexible, lightweight, and complex-shaped piezoelectric devices by 3D printing (Figure 9e). The d_{31} coefficients were measured to be about 18 pC/N. PVDF films with enhanced β-phase percentage[139] were fabricated by 3D printing (Figure 9f).

This section reviews the common preparation methods for PVDF. The different fabrication methods and polarization of PVDF are shown in Table 2. The electrospinning process has the advantages of direct polarization, while spin coating and pouring methods are simpler and more compatible with other processes. As a new technology, 3D printing has also attracted the attention of researchers.

Table 2. Different fabrication methods and polarization of PVDF

Material	Performance	Fabrication method	Poling conditions
PVDF[134] (PDMS / Ag)	peak-to-peak voltage Vp-p= 2.2 V Piezoelectric performance is not greatly affected by bending cycle	Electrospinning (dissolve PVDF in 1.5 mL DMF and 3.5 mL acetone)	No Poling

Preprints (www.preprints.org) | NOT PEER-REVIEWED | Posted: 9 November 2020 doi:10.20944/preprints202011.0262.v1

PVDF[106] (PVDF/AG)	peak-to-peak voltage Vp-p= 4.6 V 200 times higher than randomly aligned PVDF nanofiber	Electrospinning (2000 rpm and needle tip-to-collector distance is 4 cm)	No Poling
P(VDF-TrFE)[97] (BTO)/P(VDF-TrFE)	able to distinguish and sense the energy of a free-falling ball as low as 0.6 μJ and movement of walking ants	Electrospinning (135 °C for 2 h)	No Poling
PVDF[9] (PVDF/ BNT-ST)	the measurement system of the output voltage as a function of frequency	Electrospinning (feed rate of 1.0 ml/hour needle tip to collector distance is 10 cm humidity of 25 ~ 40%)	No Poling
PVDF[136] (PVDF/BT/graphene)	peak-to-peak voltage Vp-p= 11 V nanocomposite fibers are promising for wearable devices.	Electrospinning (feed rate of 0.5 ml/hour 2000 rpm and needle tip to collector distance is 12 cm for 3 h)	No Poling
PVDF–TrFE[129]	d_{33} =72.2 pC/ N the piezoelectricity of thin films reaches as high as 14.0 pm/V	Spin coated the PVDF –TrFE dissolved in MEK and hot embossed the silicon mold on the film	DC poling (Electric voltage varied from 30 to 60 V and the temperature was 90 or 110 ℃)
PVDF-TrFE[130]	d_{33} =38-74 pC/ N	Spin-coated PVDF–TrFE into thin films to Induce the formation of β phase	No Poling
PVDF–TrFE[132]	d_{33} = 20 pC/ N	Solvent Casting PVDF–TrFE for 20 μm thickness under the effect of electrode poling	electrode poling (electric field is 75 MV /m)

PVDF[61] (PVDF/PZT)	d_{33} = 60-84 pC/ N	Solution Casting PVDF/PZT to fabricate Piezoelectric composite films	No Poling The higher the content of PZT ceramic, the greater the proportion of β phase of PVDF
PVDF[140] (PVDF/BaTiO3)	the piezoelectric response of the PVDF/ BaTiO3 nanocomposite is found three times higher than nanocomposite fabricated by solvent casted more homogeneous dispersion's PVDF/ BaTiO3 nanocomposites than that fabricated by solvent casted.	3D print	Thermal poling (performed for 2 h)
PVDF[137]	thin films became very dense with high β-phase after depositing layer-by-layer.	3D print	No Poling （carbon nanotubes were added as a nucleating agent to induce the formation of β phase state of PVDF）
PVDF[138]	d31 =18 pC/N	3D print	No Poling
PVDF[139]	piezoelectric PVDF films with enhanced β-phase percentage	3D print	corona poling

4. Flexible Electromechanical Device Made by PVDF

PVDF polymer material has the advantages of low weight, high flexibility, high sensitivity, good fit and ductility, and high piezoelectric coefficient. It is suitable for flexible sensors with high flexibility requirements and is used in physics, chemistry, and biology. These fields have a wide range of applications.

Preprints (www.preprints.org) | NOT PEER-REVIEWED | Posted: 9 November 2020 doi:10.20944/preprints202011.0262.v1

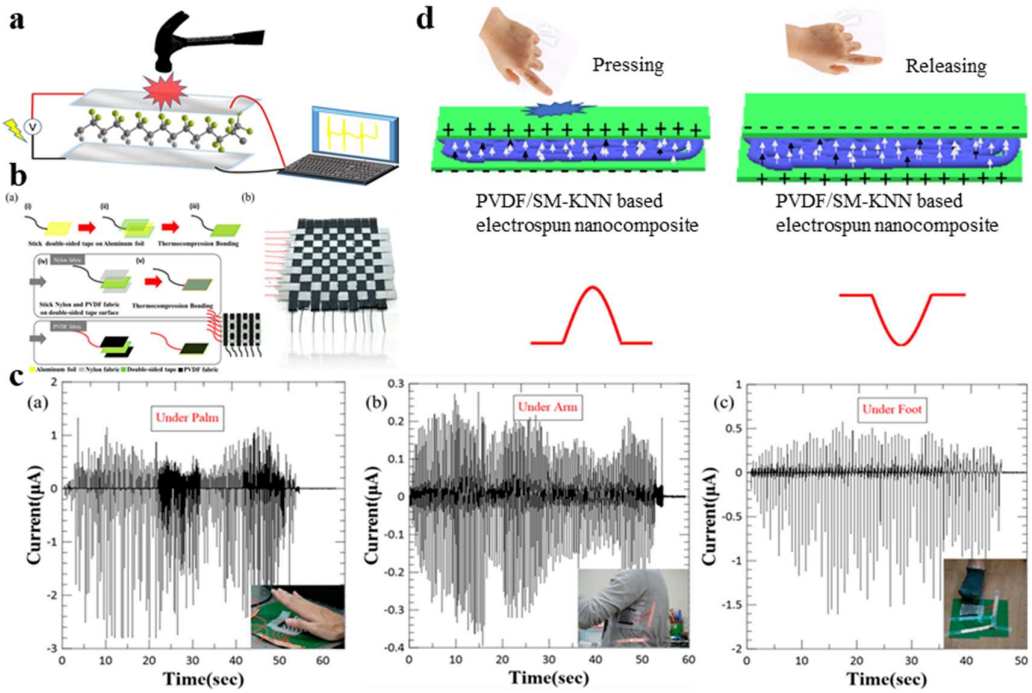

Figure 10. (a) Schematic of the energy harvesting device; **(b)** Schematic diagram of woven triboelectric nanogenerator production process[141]; **(c)** Nanogenerator harvests energy from human finger tapping, human arm movement and human footsteps[141]; **(d)** The phenomenon of charge separation during the process of press nanogenerator and release pressure of nanogenerator[142].

4.1. Energy Harvesting Device

The main principle of energy harvesting device manufacturing is to use the piezoelectric conversion effect of piezoelectric materials. Under external pressure, the piezoelectric material deforms and generates a voltage, thereby generating energy. A schematic diagram of the energy harvesting device is shown in Figure 10a. In 2020, Mokhtari et al.[143] fabricated a high-performance hybrid piezofiber composed of a PVDF and barium titanate (BT) nanoparticle (mass ratio 10:1). These fibers are knitted to fabricate a wearable energy generator with a power density of 87 μW cm^{-3} and a maximum voltage output of 4 V. In 2019, Sang et al.[144] prepared a wearable piezoelectric energy harvester based on core-shell piezoelectric yarns prepared by twining the yarns around a conductive thread. The yarns were composed of flexible piezoelectric nanofibers of BNT-ST and PVDF-TrFE by electrospinning. Muhammad et al.[141] fabricated a woven triboelectric nanogenerator using commercial nylon cloth and PVDF nanofibers, which can harvest energy from human motions. A woven triboelectric nanogenerator harvests energy from human movement; a schematic diagram of the production process of this device is shown in Figure 10b. Figure 10c shows that the nanogenerator harvests energy from human finger tapping, human arm movement, and human footsteps. Satyaranjan et al.[142] fabricated a nanogenerator based on flexible PVDF/SM-KNN, which has a current density of 5.5 mA/cm^2 and a power density of 115.5 mw/cm^2. Figure 10d shows the charge separation phenomenon during the pressing process and the release pressure of the nanogenerator.

4.2. Physical Sensors

In sensing applications, flexible and wearable pressure sensors are made of piezoelectric polymer materials with flexible characteristics. High-voltage electrospinning can be used to fabricate PVDF piezoelectric nanofiber films[51,145-149]. Gong et al.[134] combined the PVDF nanofiber membrane by electrospinning with PDMS-Ag NWS and PET/ITO electrodes to fabricate sensors (Figure 11a)[134]. This type of sensor has evident piezoelectric properties and performs well in quantitative pressure measurement. In addition, because of their shape-preserving function, they can

Preprints (www.preprints.org) | NOT PEER-REVIEWED | Posted: 9 November 2020 doi:10.20944/preprints202011.0262.v1

be used as real-time monitors of people's activities (Figure 11b). Lee et al.[94] proposed a highly sensitive gauge sensor based on PVDF and ZnO nanostructures on graphene electrodes (Figure 11c)[94]. It can detect pressure changes with the lowest 10 Pa value, which is 1000 times lower than the minimum required for artificial skin. The temperature value calculation is based on the signal recovery time (Figure 11d). The PVDF-TrFE copolymer membrane pressure sensor is manufactured via a standard photolithography process that can be used for batch processing, thereby reducing costs. The resulting membrane has good uniformity and high polymer pattern resolution[150]. Alluri et al.[68] processed piezoelectric films made of PVDF and $BaTi_{(1-x)}ZrxO_3$, which can effectively convert pressure signals into electrical signals, with a maximum peak power of 15.8 nW. The 3D printed PVDF with $BaTiO_3$ (BTO) filler[151] can also be used for pressure sensing[151]. Compared with the single PVDF composite of TNL[152-154], the sensitivity was increased by 333.46% at 5 kPa under the effects of the new additives shape, good interaction, and well-distributed hybrid additives in the matrix. This confirmed that it was possible to fabricate low-cost and lightweight electronic devices with reduced quantities of metal oxides and pressure sensing devices.

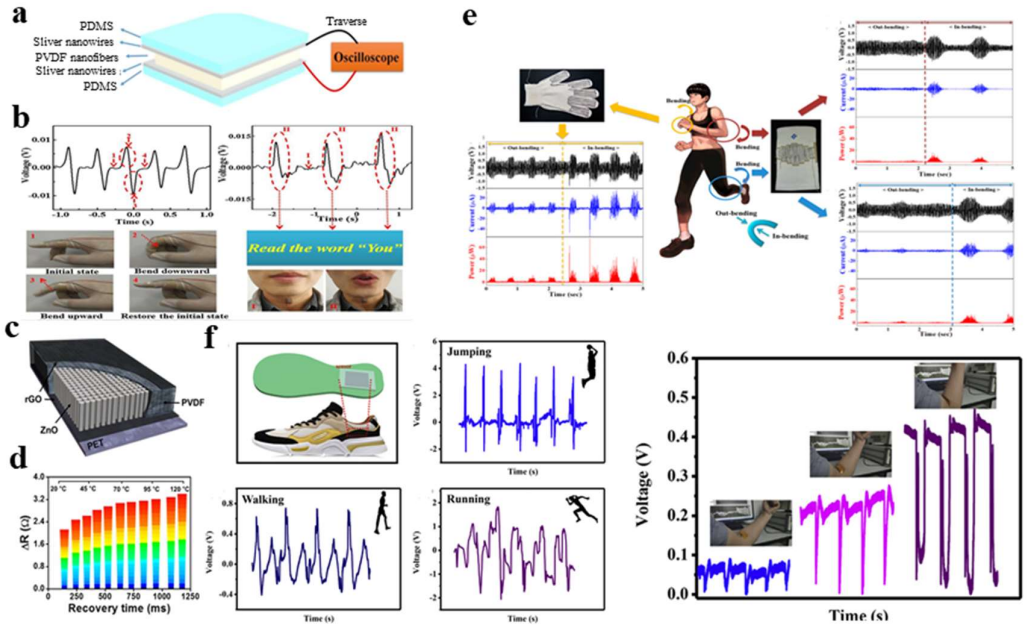

Figure 11. (a) Schematic of flexible pressure sensor used to detect pressure signal[134]; **(b)** device was used as a motion sensor to monitor knuckle bends and vocal cord vibrates[134]; **(c)** Schematic of sensor based on PVDF and ZnO nanostructures on graphene electrodes[94]; **(d)** The relationship between temperature and recovery time[94]; **(e)** Generated output voltages, output currents, output powers by Finger bending, knee and elbow movements[144]; **(f)** Pressure sensor embedded in the bottom of the insole or stuck on human arm and voltage generated by jumping, walking, running and different bending angles' elbows[123].

Sang et al.[144] manufactured a wearable piezoelectric energy harvester by electrospinning PVDF-TrFE and BNT-ST($0.78Bi_{0.5}Na_{0.5}TiO_3$-$0.22SrTiO_3$). The generated output voltages, output currents, output powers by finger bending, and knee and elbow movements are shown in Figure 11e. Ye et al.[123] fabricated flexible wearable pressure sensors that were sensitive to various human behaviors based on piezoelectric materials. The pressure sensor was embedded in the bottom of the insole or stuck on the human arm, and the voltage generated by jumping, walking, running, and elbows at different bending angles is shown in Figure 11f.

4.3. Chemical sensor based on piezoelectric polymer

As a flexible piezoelectric material, the mechanical deformation state of PVDF electrically driven is directly related to its mass load. Then, by modifying the sensitive surface with adsorbent materials,

Preprints (www.preprints.org) | NOT PEER-REVIEWED | Posted: 9 November 2020 doi:10.20944/preprints202011.0262.v1

it can specifically adsorb gas or water vapor to form a mass sensor. For example, when the sensing interface contacts the target gas, the physical shape and mass changes caused by the absorption of gas will affect the resonance frequency and other physical parameters of the piezoelectric polymer-sensitive film. To detect the hydrogen concentration, Zengwei et al.[155] applied the phase separation method to deposit a PVDF microporous membrane on the surface of a palladium-loaded tin dioxide (Pd-SnO_2) gas-sensitive film. The stability of the sensor under high humidity was evidently improved by the influence of the PVDF microporous membrane. Hydrogen sensor[156] can be made by sticking the Pd film on both sides of the PVDF membrane. Because of the selective absorption of hydrogen by the palladium membrane, expansion deformation occurs under the PVDF action, which is converted into voltage signal output.

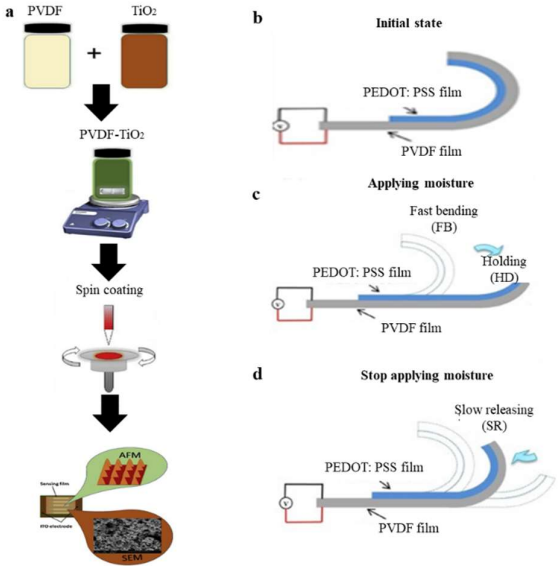

Figure 12. (a) Schematic of the spin coated PVDF-TiO_2 on interdigital ITO electrode[157]; **(b-d)** Graphical representation of the PEDOT: PSS/PVDF generator producing a stable DC voltage.

The introduction of humidity in sensitive materials can also play a role in humidity sensing. The spin coating technique was used to prepare the PVDF TiO_2 nanocomposite films on interdigital ITO electrode[157], and the surface morphology was modified by acetone etching. The volume deformation of PVDF is caused by the hygroscopicity of nano-TiO_2, resulting in a piezoelectric effect (Figure 12a)[157]. Wang et al.[158] proposed a simple and low-cost method to prepare a moisture-responsive composite membrane composed of PEDOT: PSS and PVDF by spin coating and thermal evaporation. The bending angles of the composite film in both directions can reach 191 and 225, respectively, showing good bidirectional bending performance. As shown in Figure 12b-d, the PVDF film is glued together with the PEDOT: PSS film. PEDOT: PSS easily absorbs water[159-161]. In different humidity environments, PEDOT has different bending degrees due to different water absorption rates. PVDF films produce voltage signals under the corresponding bending degrees, representing the specific humidity.

4.4. Biosensor and bionic actuator based on piezoelectric polymer

Piezoelectric polymers are used as biosensors mainly through biosensor surface modification. The binding of biological target molecules on the sensing surface changes the mass of the sensing end of the sensor, thus affecting the resonant output of the piezoelectric polymer. PVDF-TrFE films were fabricated by electrodeposition, and piezoelectric polymer ultrasonic transceivers were developed, which proved that they can be used for the ultra-sensitive detection of antibiotics. The diameter of the entire ultrasonic transceiver was 680 μm. The ultrasonic transducers consist of a receiver and a transmitter, which is patterned on a gold electrode and integrated with a microfluidic channel. The

Preprints (www.preprints.org) | NOT PEER-REVIEWED | Posted: 9 November 2020 doi:10.20944/preprints202011.0262.v1

biosensor was successfully applied to detect the animals' doxycycline with a detection limit of 50 ppb (Figure 13a-c)[162]. In the field of microfluidic channels, the developed on-chip ultrasonic transducer was performed excellently, with the potential to be used for ultra-sensitive detection of DNA, proteins, and food antibiotics. Lin et al.[163] fabricated microporous PVDF membranes with different surface morphologies from coagulation baths of different strengths by immersion-precipitation. Using the dual-step procedure, ss-DNA was covalently immobilized on the membranes. The antibody in serum can be effectively adsorbed by the immobilized DNA, performing antibody detection. Similarly, nucleic acid sensors based on PVDF[164] have been developed. In the experiment, they used the hybridization between the capture probe and target analyte (Figure 13d)[164] and found that the mass load on the membrane was proportional to the quantity of target nucleic acids (Figure 13e)[164].

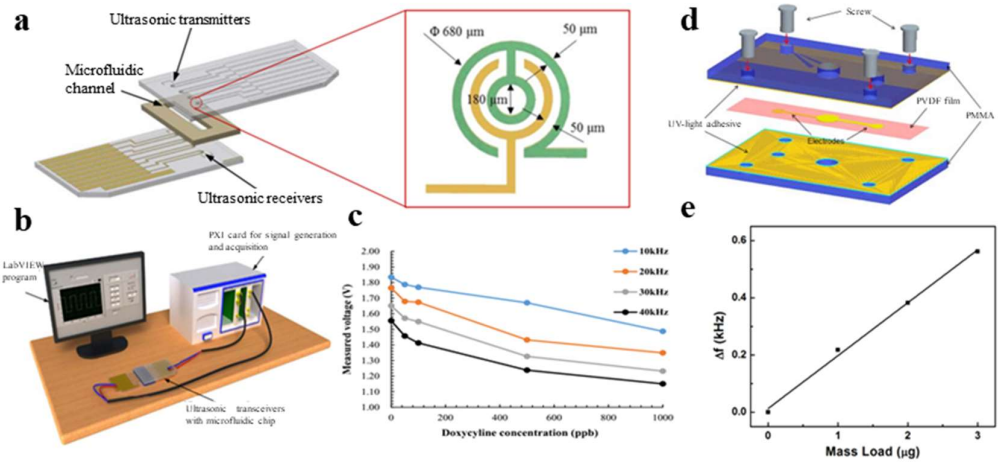

Figure 13. (a) Schematic of the chip[162]; **(b)**The experimental setup for characterizing the ultrasonic transceivers[162]; **(c)**The plastic microfluidic chip with ultrasonic transceivers[162]; **(d)** Schematic of the biosensor using PVDF film as piezoelectric layer[164]; **(e)** Relationship between mass load and frequency shift (Δf)[164].

In recent years, much attention has been paid to the research of artificial bionics devices. In 2019, Wu et al.[165] reported a flexible robot based on a piezoelectric single chip bending structure (Figure 14a-b)[165]. Its relative speed is 20 times its body length per second, which is the fastest measurement speed among the reported artificial robots on an insect scale. The soft robot uses the principle of several kinds of animal movements, such as carrying load, the firmness of a cockroach, and climbing slopes. Even after bearing the weight of an adult's footsteps (approximately 1 million times heavier than the robot), the system can continue to move (Figure 14c)[165].

Piezoelectric polymers also have good performance in the manufacturing of artificial muscles. Simaite et al.[166] prepared a hybrid membrane with hydrophilic PVDF grafted poly- (ethylene glycol) monomethyl ether methacrylate (PEGMA) outer surface and hydrophobic main body, which is a model human muscle composition, as shown in Figure 14d . The results are expected to be used in artificial muscles. Xiao et al.[167] fabricated a fish-like robot to imitate fish swimming. The fish-like robot is composed of a body and a tail. The body is made of expandable polystyrene and the tail is made of graphene-PVDF as an actuator. The graphene-PVDF film is connected with a flexible Au wire. When the power is turned on, the fish's tail is bent, and when the power is turned off, the tail returns to its original position. As the power is continuously turned on and off, the fish-shaped robot can move forward as a speed of 5.02 mm/s. Kim et al.[168] fabricated a new IPMC actuator on the basis of blend membrane made by PVDF/ polyvinyl pyrrolidone/ /polystyrene sulfuric acid . The robot can support 2-, 4-, or 6-IPMC-leg models and this miniature walking robot has a size of 18 x 11 x 12 mm, a weight of 1.3g and a maximum speed of 0.58mm/s.

Preprints (www.preprints.org) | NOT PEER-REVIEWED | Posted: 9 November 2020 doi:10.20944/preprints202011.0262.v1

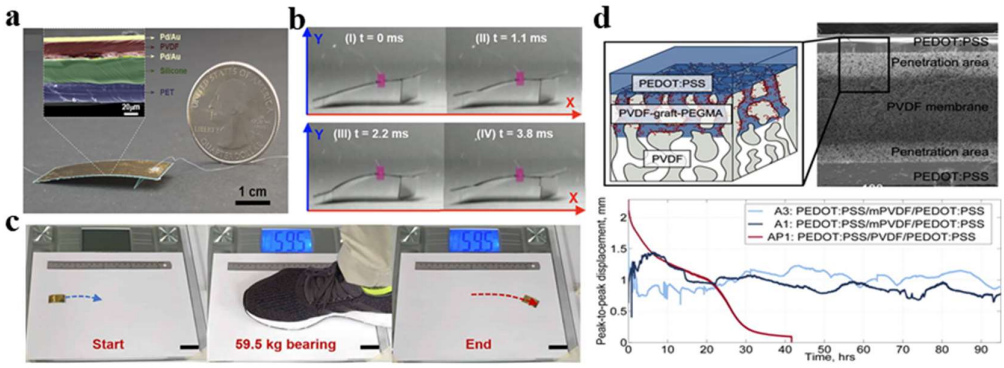

Figure 14. (a) Optical photo of the fabricated robot and the SEM image of the cross-sectional view of the prototype robot with different layers of materials[165]; **(b)** Images of prototype robot the movements in a driving cycled[165]; **(c)** After bearing the weight of an adult's footsteps (about 1 million times heavier than the robot), the system can continue to move[165]. **(d)** The cross-sectional view of the hydrophilic PVDF-graft-PEGMA[166].

5. Conclusion and perspectives

Although inorganic piezoelectric materials have the advantages of a large piezoelectric coefficient and high strength, they are fragile and unsuitable for applications with higher flexibility requirements. As a typical representative of flexible piezoelectric polymers, PVDF has irreplaceable advantages in the development of piezoelectric materials. It has great flexibility and can also improve its piezoelectric properties by doping optimization or other processes. Various doping methods for PVDF polymer materials have been introduced, and the effects of different piezoelectric materials, nanomaterials, and biomaterials were compared. Some preparation methods for improving the polarization properties of piezoelectric polymers have also been introduced in detail. Based on flexible piezoelectric polymer materials, we can obtain flexible electromechanical devices for different purposes, such as energy harvesting devices, chemical sensor for humidity, pressure, gas, and biomolecules.

We can prepare actuators of different sizes and functions based on flexible piezoelectric polymer materials. However, it is still less than the conversion coefficient of the inorganic piezoelectric material. In the follow-up work, the optimization method of the piezoelectric polymer should continue to be studied and applied to wearable devices. 1) Piezoelectric materials based on biological crystals are one of the materials with great potential. The modification of the unique functional groups of biological materials can be used to improve the vertical piezoelectric coefficient of PVDF. 2) Aiming at shape retention, the method of preparing flexible electromechanical devices with high mechanical voltage conversion efficiency should be further explored. 3) In addition, the use of piezoelectric polymer materials for wearable flexible devices requires the piezoelectric polymer exhibiting better skin affinity, more compatibility with other flexible materials to be suitable for the applications of physiological index sensors and implantable devices. Biomaterials and flexible conductive polymers can be introduced to improve its biocompatibility，antifouling ability, and the ability of integration with hydrophilic surface. In summary, giving full play to the flexible characteristics of piezoelectric polymers and developing wearable piezoelectric sensors and executable devices will have very broad application prospects.

Author Contributions: Conceptualization, S.G. and X.D.; investigation, S.G. and Q.X.; writing-original draft preparation, S.G, Q.X. and X.D.; writing-review and editing, S.G, Q.X., X.D. and M.X.; supervision, Q.X. and K.C.A; funding acquisition, Q.X. and X.D. All authors have read and agreed to the published version of the manuscript.

Funding: This research was funded by the National Natural Science Foundation of China, grant number 61674114, 91743110, 21861132001; by National Key R&D Program of China, grant number 2017YFF0204604, 2018YFE0118700; by Tianjin Applied Basic Research and Advanced Technology, grant number 17JCJQJC43600;

by the 111 Project, grant number B07014; and the Initial Scientific Research Fund of State Key Laboratory of Precision Measuring Technology and Instruments, Tianjin University, grant number Pilq1902. The authors thank the Foundation for Talent Scientists of Nanchang Institute for Micro-technology of Tianjin University.

Conflicts of Interest: The authors declare no conflict of interest.

References

1. Neppiras, E.A. Piezoelectric ceramics 1971 B. Jaffe, W. R. Cook Jr and H. Jaffe. London and New York: Academic Press. 317 pp., #5.50. *Journal of Sound & Vibration* **1972**, *20*, 562-563.
2. Rao, K.S.; Sateesh, J.; Guha, K.; Baishnab, K.L.; Ashok, P.; Sravani, K.G. Design and analysis of MEMS based piezoelectric micro pump integrated with micro needle. *Microsystem Technologies-Micro-and Nanosystems-Information Storage and Processing Systems* **2020**, *26*, 3153-3159, doi:10.1007/s00542-018-3807-4.
3. Liu, J.; Zuo, H.; Xia, W.; Luo, Y.; Yao, D.; Chen, Y.; Wang, K.; Li, Q. Wind energy harvesting using piezoelectric macro fiber composites based on flutter mode. *Microelectronic Engineering* **2020**, *231*, doi:10.1016/j.mee.2020.111333.
4. Kaneko, R.; Froemel, J.; Tanaka, S. Development of PVDF-TrFE/SiO2 composite film bulk acoustic resonator. *Sensors and Actuators a-Physical* **2018**, *284*, 120-128, doi:10.1016/j.sna.2018.10.025.
5. Wang, Y.; Zhu, X.; Zhang, T.; Bano, S.; Pan, H.; Qi, L.; Zhang, Z.; Yuan, Y. A renewable low-frequency acoustic energy harvesting noise barrier for high-speed railways using a Helmholtz resonator and a PVDF film. *Applied Energy* **2018**, *230*, 52-61, doi:10.1016/j.apenergy.2018.08.080.
6. Kaneko, R.; Froemel, J.; Tanaka, S.; Ieee. PVDF-TrFE/SiO2 Composite Film Bulk Acoustic Resonator for Frequency-Modulated Sensor Application. In *2018 Ieee International Ultrasonics Symposium*, 2018.
7. Lee, H.Y.; Choi, B. A multilayer PVDF composite cantilever in the Helmholtz resonator for energy harvesting from sound pressure. *Smart Materials and Structures* **2013**, *22*, doi:10.1088/0964-1726/22/11/115025.
8. Li, B.; Laviage, A.J.; You, J.H.; Kim, Y.-J. Harvesting low-frequency acoustic energy using multiple PVDF beam arrays in quarter-wavelength acoustic resonator. *Applied Acoustics* **2013**, *74*, 1271-1278, doi:10.1016/j.apacoust.2013.04.015.
9. Ji, S.H.; Cho, J.H.; Jeong, Y.H.; Paik, J.-H.; Yun, J.D.; Yun, J.S. Flexible lead-free piezoelectric nanofiber composites based on BNT-ST and PVDF for frequency sensor applications. *Sensors and Actuators a-Physical* **2016**, *247*, 316-322, doi:10.1016/j.sna.2016.06.011.
10. Koc, M.; Parali, L.; San, O. Fabrication and vibrational energy harvesting characterization of flexible piezoelectric nanogenerator (PEN) based on PVDF/PZT. *Polymer Testing* **2020**, *90*, doi:10.1016/j.polymertesting.2020.106695.
11. Chamankar, N.; Khajavi, R.; Yousefi, A.A.; Rashidi, A.; Golestanifard, F. A flexible piezoelectric pressure sensor based on PVDF nanocomposite fibers doped with PZT particles for energy harvesting applications. *Ceramics International* **2020**, *46*, 19669-19681, doi:10.1016/j.ceramint.2020.03.210.
12. Yadav, P.; Raju, T.D.; Badhulika, S. Self-Poled hBN-PVDF Nanofiber Mat-Based Low-Cost, Ultrahigh-Performance Piezoelectric Nanogenerator for Biomechanical Energy Harvesting. *Acs Applied Electronic Materials* **2020**, *2*, 1970-1980, doi:10.1021/acsaelm.0c00272.
13. Polat, K. Energy harvesting from a thin polymeric film based on PVDF-HFP and PMMA blend. *Applied Physics a-Materials Science & Processing* **2020**, *126*, doi:10.1007/s00339-020-03698-w.
14. Shehata, N.; Hassanin, A.H.; Elnabawy, E.; Nair, R.; Bhat, S.A.; Kandas, I. Acoustic Energy Harvesting and Sensing via Electrospun PVDF Nanofiber Membrane. *Sensors* **2020**, *20*, doi:10.3390/s20113111.
15. Zhang, Q.; Sanchez-Fuentes, D.; Desgarceaux, R.; Escofet-Majoral, P.; Oro-soler, J.; Gazquez, J.; Larrieu, G.; Chariot, B.; Gomez, A.; Gich, M., et al. Micro/Nanostructure Engineering of Epitaxial Piezoelectric alpha-Quartz Thin Films on Silicon. *Acs Applied Materials & Interfaces* **2020**, *12*, 4732-4740, doi:10.1021/acsami.9b18555.
16. Zhang, H.; Yao, Y.; Shi, Y. Performance Enhancement of Interdigital Electrode-Piezoelectric Quartz Crystal (IDE-PQC) Salt Concentration Sensor by Increasing the Electrode Area of Piezoelectric Quartz Crystal (PQC). *Sensors* **2018**, *18*, doi:10.3390/s18103224.
17. Shibata, K.; Wang, R.P.; Tou, T.; Koruza, J. Applications of lead-free piezoelectric materials. *Mrs Bulletin* **2018**, *43*, 612-616, doi:10.1557/mrs.2018.180.
18. Panda, P.K. Review: environmental friendly lead-free piezoelectric materials. *Journal of Materials Science* **2009**, *44*, 5049-5062, doi:10.1007/s10853-009-3643-0.

19. Kim, H.S.; Kim, J.H.; Kim, J. A Review of Piezoelectric Energy Harvesting Based on Vibration. *International Journal of Precision Engineering and Manufacturing* **2011**, *12*, 1129-1141, doi:10.1007/s12541-011-0151-3.
20. Polsongkram, D.; Chamninok, P.; Pukird, S.; Chow, L.; Lupan, O.; Chai, G.; Khallaf, H.; Park, S.; Schulte, A. Effect of synthesis conditions on the growth of ZnO nanorods via hydrothermal method. *Physica B-Condensed Matter* **2008**, *403*, 3713-3717, doi:10.1016/j.physb.2008.06.020.
21. Li, H.; Tian, C.; Deng, Z.D. Energy harvesting from low frequency applications using piezoelectric materials. *Applied Physics Reviews* **2014**, *1*, doi:10.1063/1.4900845.
22. Khadtare, S.; Ko, E.J.; Kim, Y.H.; Lee, H.S.; Moon, D.K. A flexible piezoelectric nanogenerator using conducting polymer and silver nanowire hybrid electrodes for its application in real-time muscular monitoring system. *Sensors and Actuators a-Physical* **2019**, *299*, doi:10.1016/j.sna.2019.111575.
23. Pan, Q.; Xiong, Y.-A.; Sha, T.-T.; You, Y.-M. Recent progress in the piezoelectricity of molecular ferroelectrics. *Materials Chemistry Frontiers* **2020**, 10.1039/D0QM00288G, doi:10.1039/D0QM00288G.
24. Crainic, T.G.; Perboli, G.; Mancini, S.; Tadei, R. Two-Echelon Vehicle Routing Problem: A satellite location analysis. In *6th International Conference on City Logistics*, Tanguchi, E., Thompson, R.G., Eds. 2010; Vol. 2, pp. 5944-5955.
25. Qin, C.; Gu, Y.; Sun, X.; Wang, X.; Zhang, Y. Structural dependence of piezoelectric size effects and macroscopic polarization in ZnO nanowires: A first-principles study. *Nano Research* **2015**, *8*, 2073-2081, doi:10.1007/s12274-015-0718-x.
26. Zheng, D.; Roumanille, P.; Hermet, P.; Cambon, M.; Haines, J.; Cambon, O. Enhancement of the piezoelectric effect in Fe-substituted GaAsO4: A combined XRD, Raman spectroscopy and first principles study. *Solid State Sciences* **2020**, *101*, doi:10.1016/j.solidstatesciences.2020.106157.
27. He, J.; Wen, T.; Qian, S.; Zhang, Z.; Tian, Z.; Zhu, J.; Mu, J.; Hou, X.; Geng, W.; Cho, J., et al. Triboelectric-piezoelectric-electromagnetic hybrid nanogenerator for high-efficient vibration energy harvesting and self-powered wireless monitoring system. *Nano Energy* **2018**, *43*, 326-339, doi:10.1016/j.nanoen.2017.11.039.
28. Wang, P.; Pan, L.; Wang, J.; Xu, M.; Dai, G.; Zou, H.; Dong, K.; Wang, Z.L. An Ultra-Low-Friction Triboelectric-Electromagnetic Hybrid Nanogenerator for Rotation Energy Harvesting and Self-Powered Wind Speed Sensor. *Acs Nano* **2018**, *12*, 9433-9440, doi:10.1021/acsnano.8b04654.
29. Wang, W.; Xu, J.; Zheng, H.; Chen, F.; Jenkins, K.; Wu, Y.; Wang, H.; Zhang, W.; Yang, R. A spring-assisted hybrid triboelectric-electromagnetic nanogenerator for harvesting low-frequency vibration energy and creating a self-powered security system. *Nanoscale* **2018**, *10*, 14747-14754, doi:10.1039/c8nr04276d.
30. Yuan, Y.; Zhang, H.; Wang, J.; Xie, Y.; Khan, S.A.; Jin, L.; Yan, Z.; Huang, L.; Pan, T.; Yang, W., et al. Hybrid nanogenerators for low frequency vibration energy harvesting and self-powered wireless locating. *Materials Research Express* **2018**, *5*, doi:10.1088/2053-1591/aaa563.
31. Zhang, H.; Yang, Y.; Su, Y.; Chen, J.; Adams, K.; Lee, S.; Hu, C.; Wang, Z.L. Triboelectric Nanogenerator for Harvesting Vibration Energy in Full Space and as Self- Powered Acceleration Sensor. *Advanced Functional Materials* **2014**, *24*, 1401-1407, doi:10.1002/adfm.201302453.
32. Invernizzi, F.; Dulio, S.; Patrini, M.; Guizzetti, G.; Mustarelli, P. Energy harvesting from human motion: materials and techniques. *Chemical Society Reviews* **2016**, *45*, 5455-5473, doi:10.1039/C5CS00812C.
33. Zhang, Q.M.; Bharti, V.; Kavarnos, G.; Schwartz, M. *Poly(Vinylidene Fluoride) (PVDF) and its Copolymers*; American Cancer Society: 2002; 10.1002/0471216275.esm063.
34. Martins, P.; Lopes, A.C.; Lanceros-Mendez, S. Electroactive phases of poly(vinylidene fluoride): Determination, processing and applications. *Progress in Polymer Science* **2014**, *39*, 683-706, doi:10.1016/j.progpolymsci.2013.07.006.
35. Ameduri, B. From Vinylidene Fluoride (VDF) to the Applications of VDF-Containing Polymers and Copolymers: Recent Developments and Future Trends. *Chemical Reviews* **2009**, *109*, 6632-6686, doi:10.1021/cr800187m.
36. Shepelin, N.A.; Glushenkov, A.M.; Lussini, V.C.; Fox, P.J.; Dicinoski, G.W.; Shapter, J.G.; Ellis, A.V. New developments in composites, copolymer technologies and processing techniques for flexible fluoropolymer piezoelectric generators for efficient energy harvesting. *Energy & Environmental Science* **2019**, *12*, 1143-1176, doi:10.1039/C8EE03006E.
37. Fang, J.; Wang, X.; Lin, T. Electrical power generator from randomly oriented electrospun poly(vinylidene fluoride) nanofibre membranes. *Journal of Materials Chemistry* **2011**, *21*, 11088-11091, doi:10.1039/c1jm11445j.

38. Huang, F.; Wei, Q.; Cai, Y. Surface structures and contact angles of electrospun poly(vinylidene fluoride) nanofiber membranes. *International Journal of Polymer Analysis and Characterization* **2008**, *13*, 292-301, doi:10.1080/10236660802190963.
39. Pan, C.-T.; Yen, C.-K.; Wang, S.-Y.; Lai, Y.-C.; Lin, L.; Huang, J.C.; Kuo, S.-W. Near-field electrospinning enhances the energy harvesting of hollow PVDF piezoelectric fibers. *Rsc Advances* **2015**, *5*, 85073-85081, doi:10.1039/c5ra16604g.
40. Liu, Z.H.; Pan, C.T.; Lin, L.W.; Huang, J.C.; Ou, Z.Y. Direct-write PVDF nonwoven fiber fabric energy harvesters via the hollow cylindrical near-field electrospinning process. *Smart Materials and Structures* **2014**, *23*, doi:10.1088/0964-1726/23/2/025003.
41. Zhu, G.; Zeng, Z.; Zhang, L.; Yan, X. Piezoelectricity in beta-phase PVDF crystals: A molecular simulation study. *Computational Materials Science* **2008**, *44*, 224-229, doi:10.1016/j.commatsci.2008.03.016.
42. Hoeher, R.; Raidt, T.; Novak, N.; Katzenberg, F.; Tiller, J.C. Shape-Memory PVDF Exhibiting Switchable Piezoelectricity. *Macromolecular Rapid Communications* **2015**, *36*, 2042-2046, doi:10.1002/marc.201500410.
43. Chang, C.; Tran, V.H.; Wang, J.; Fuh, Y.-K.; Lin, L. Direct-Write Piezoelectric Polymeric Nanogenerator with High Energy Conversion Efficiency. *Nano Letters* **2010**, *10*, 726-731, doi:10.1021/nl9040719.
44. Persano, L.; Dagdeviren, C.; Su, Y.; Zhang, Y.; Girardo, S.; Pisignano, D.; Huang, Y.; Rogers, J.A. High performance piezoelectric devices based on aligned arrays of nanofibers of poly(vinylidenefluoride-co-trifluoroethylene). *Nature Communications* **2013**, *4*, doi:10.1038/ncomms2639.
45. Pi, Z.; Zhang, J.; Wen, C.; Zhang, Z.-b.; Wu, D. Flexible piezoelectric nanogenerator made of poly(vinylidenefluoride-co-trifluoroethylene) (PVDF-TrFE) thin film. *Nano Energy* **2014**, *7*, 33-41, doi:10.1016/j.nanoen.2014.04.016.
46. Zhang, L.; Yu, X.; You, S.; Liu, H.; Zhang, C.; Cai, B.; Xiao, L.; Liu, W.; Guo, S.; Zhao, X. Highly sensitive microfluidic flow sensor based on aligned piezoelectric poly(vinylidene fluoride-trifluoroethylene) nanofibers. *Applied Physics Letters* **2015**, *107*, doi:10.1063/1.4937733.
47. Choi, K.; Lee, S.C.; Liang, Y.; Kim, K.J.; Lee, H.S. Transition from Nanorod to Nanotube of Poly(vinylidene trifluoroethylene) Ferroelectric Nanofiber. *Macromolecules* **2013**, *46*, 3067-3073, doi:10.1021/ma302679g.
48. Gui, J.; Zhu, Y.; Zhang, L.; Shu, X.; Liu, W.; Guo, S.; Zhao, X. Enhanced output-performance of piezoelectric poly(vinylidene fluoride trifluoroethylene) fibers-based nanogenerator with interdigital electrodes and well-ordered cylindrical cavities. *Applied Physics Letters* **2018**, *112*, doi:10.1063/1.5019319.
49. Oh, S.R.; Yao, K.; Chow, C.L.; Tay, F.E.H. Residual stress in piezoelectric poly(vinylidene-fluoride-co-trifluoroethylene) thin films deposited on silicon substrates. *Thin Solid Films* **2010**, *519*, 1441-1444, doi:10.1016/j.tsf.2010.09.042.
50. Shao, H.; Fang, J.; Wang, H.; Lin, T. Effect of electrospinning parameters and polymer concentrations on mechanical-to-electrical energy conversion of randomly-oriented electrospun poly(vinylidene fluoride) nanofiber mats. *Rsc Advances* **2015**, *5*, 14345-14350, doi:10.1039/c4ra16360e.
51. Lang, C.; Fang, J.; Shao, H.; Wang, H.; Yan, G.; Ding, X.; Lin, T. High-output acoustoelectric power generators from poly(vinylidenefluoride-co-trifluoroethylene) electrospun nano-nonwovens. *Nano Energy* **2017**, *35*, 146-153, doi:10.1016/j.nanoen.2017.03.038.
52. Soin, N.; Shah, T.H.; Anand, S.C.; Geng, J.; Pornwannachai, W.; Mandal, P.; Reid, D.; Sharma, S.; Hadimani, R.L.; Bayramol, D.V., et al. Novel "3-D spacer" all fibre piezoelectric textiles for energy harvesting applications. *Energy & Environmental Science* **2014**, *7*, 1670-1679, doi:10.1039/c3ee43987a.
53. Zirkl, M.; Sawatdee, A.; Helbig, U.; Krause, M.; Scheipl, G.; Kraker, E.; Ersman, P.A.; Nilsson, D.; Platt, D.; Bodo, P., et al. An All-Printed Ferroelectric Active Matrix Sensor Network Based on Only Five Functional Materials Forming a Touchless Control Interface. *Advanced Materials* **2011**, *23*, 2069-+, doi:10.1002/adma.201100054.
54. Yuan, Y.; Reece, T.J.; Sharma, P.; Poddar, S.; Ducharme, S.; Gruverman, A.; Yang, Y.; Huang, J. Efficiency enhancement in organic solar cells with ferroelectric polymers. *Nature Materials* **2011**, *10*, 296-302, doi:10.1038/nmat2951.
55. Kang, S.J.; Bae, I.; Shin, Y.J.; Park, Y.J.; Huh, J.; Park, S.-M.; Kim, H.-C.; Park, C. Nonvolatile Polymer Memory with Nanoconfinement of Ferroelectric Crystals. *Nano Letters* **2011**, *11*, 138-144, doi:10.1021/nl103094e.
56. Zhang, X.; Hillenbrand, J.; Sessler, G.M.; Haberzettl, S.; Lou, K. Fluoroethylenepropylene ferroelectrets with patterned microstructure and high, thermally stable piezoelectricity. *Applied Physics a-Materials Science & Processing* **2012**, *107*, 621-629, doi:10.1007/s00339-012-6840-7.
57. Liu, H.; Zhong, J.; Lee, C.; Lee, S.-W.; Lin, L. A comprehensive review on piezoelectric energy harvesting technology: Materials, mechanisms, and applications. *Applied Physics Reviews* **2018**, *5*, doi:10.1063/1.5074184.

58. Ibrahim, S.W.; Ali, W.G. A review on frequency tuning methods for piezoelectric energy harvesting systems. *Journal of Renewable and Sustainable Energy* **2012**, *4*, doi:10.1063/1.4766892.
59. Zhong, J.; Zhong, Q.; Zang, X.; Wu, N.; Li, W.; Chu, Y.; Lin, L. Flexible PET/EVA-based piezoelectret generator for energy harvesting in harsh environments. *Nano Energy* **2017**, *37*, 268-274, doi:10.1016/j.nanoen.2017.05.034.
60. Guo, H.; Wen, Z.; Zi, Y.; Yeh, M.-H.; Wang, J.; Zhu, L.; Hu, C.; Wang, Z.L. A Water-Proof Triboelectric-Electromagnetic Hybrid Generator for Energy Harvesting in Harsh Environments. *Advanced Energy Materials* **2016**, *6*, doi:10.1002/aenm.201501593.
61. Tiwari, V.; Srivastava, G. Structural, dielectric and piezoelectric properties of 0-3 PZT/PVDF composites. *Ceramics International* **2015**, *41*, 8008-8013, doi:10.1016/j.ceramint.2015.02.148.
62. Luo, C.; Yang, C.-W.; Cao, G.Z.; Shen, I.Y.; Asme. *EFFECTS OF ADDED MASS ON LEAD-ZIRCONATE-TITANATE (PZT) THIN-FILM MICROACTUATORS IN AQUEOUS ENVIRONMENTS*; 2014.
63. Pal, A.; Sasmal, A.; Manoj, B.; Rao, D.S.D.P.; Haldar, A.K.; Sen, S. Enhancement in energy storage and piezoelectric performance of three phase (PZT/MWCNT/PVDF) composite. *Materials Chemistry and Physics* **2020**, *244*, doi:10.1016/j.matchemphys.2020.122639.
64. Sabry, R.S.; Hussein, A.D. PVDF: ZnO/BaTiO3 as high out-put piezoelectric nanogenerator. *Polymer Testing* **2019**, *79*, doi:10.1016/j.polymertesting.2019.106001.
65. Sasmal, A.; Sen, S.; Devi, P.S. Frequency dependent energy storage and dielectric performance of Ba–Zr Co-doped BiFeO3 loaded PVDF based mechanical energy harvesters: effect of corona poling. *Soft Matter* **2020**, *16*, 8492-8505, doi:10.1039/D0SM01031F.
66. Li, R.; Zhao, Z.; Chen, Z.; Pei, J. Novel BaTiO3/PVDF composites with enhanced electrical properties modified by calcined BaTiO3 ceramic powders. *Materials Express* **2017**, *7*, 536-540, doi:10.1166/mex.2017.1393.
67. Kakimoto, K.-i.; Fukata, K.; Ogawa, H. Fabrication of fibrous BaTiO3-reinforced PVDF composite sheet for transducer application. *Sensors and Actuators a-Physical* **2013**, *200*, 21-25, doi:10.1016/j.sna.2013.03.007.
68. Alluri, N.R.; Saravanakumar, B.; Kim, S.-J. Flexible, Hybrid Piezoelectric Film (BaTi(1-x)ZrxO3)/PVDF Nanogenerator as a Self-Powered Fluid Velocity Sensor. *Acs Applied Materials & Interfaces* **2015**, *7*, 9831-9840, doi:10.1021/acsami.5b01760.
69. Krauss, W.; Schuetz, D.; Mautner, F.A.; Feteira, A.; Reichmann, K. Piezoelectric properties and phase transition temperatures of the solid solution of (1-x)(Bi0.5Na0.5)TiO3-xSrTiO(3). *Journal of the European Ceramic Society* **2010**, *30*, 1827-1832, doi:10.1016/j.jeurceramsoc.2010.02.001.
70. Yu, H.; Yea, Z.-G. Dielectric, ferroelectric, and piezoelectric properties of the lead-free (1-x)(Na0.5Bi0.5)TiO3-xBiAlO(3) solid solution. *Applied Physics Letters* **2008**, *93*, doi:10.1063/1.2967335.
71. Jiang, Y.; Qin, B.; Zhao, Y.; Jiang, Y.; Shi, W.; Li, Q.; Xiao, D.; Zhu, J. Phase transition, piezoelectric properties, and thermal stability of (1-x-y)BiScO3-yBiGaO(3)-xPbTiO(3) ceramics. *Journal of the American Ceramic Society* **2008**, *91*, 2943-2946, doi:10.1111/j.1551-2916.2008.02580.x.
72. Choi, S.M.; Stringer, C.J.; Shrout, T.R.; Randall, C.A. Structure and Property Investigation of a Bi-based Perovskite, Solid Solution (1x)Bi(Ni1/2Ti1/2)O3–xPbTiO3. *Journal of Applied Physics* **2005**, *98*, 5999, doi:10.1063/1.1978985
73. Lin, D.; Kwok, K.W. Structure, ferroelectric and piezoelectric properties of (Bi0.98-x La0.02Na1-x)(0.5)Ba (x) TiO3 lead-free ceramics. *Applied Physics a-Materials Science & Processing* **2009**, *97*, 229-235, doi:10.1007/s00339-009-5189-z.
74. Fu, H.X.; Cohen, R.E. Polarization rotation mechanism for ultrahigh electromechanical response in single-crystal piezoelectrics. *Nature* **2000**, *403*, 281-283, doi:10.1038/35002022.
75. Karanth, D.; Fu, H.X. Large electromechanical response in ZnO and its microscopic origin. *Physical Review B* **2005**, *72*, doi:10.1103/PhysRevB.72.064116.
76. Hernandez, B.A.; Chang, K.S.; Fisher, E.R.; Dorhout, P.K. Sol-gel template synthesis and characterization of BaTiO3 and PbTiO3 nanotubes. *Chemistry of Materials* **2002**, *14*, 480-482, doi:10.1021/cm010998c.
77. Wang, X.; Li, Y.D. Synthesis and characterization of lanthanide hydroxide single-crystal nanowires. *Angewandte Chemie-International Edition* **2002**, *41*, 4790-4793, doi:10.1002/anie.200290049.
78. Scott, J.F. Applications of modern ferroelectrics. *Science* **2007**, *315*, 954-959, doi:10.1126/science.1129564.
79. Webb, J.F. A general approach to perturbation theoretic analysis in nonlinear optics and its application to ferroelectrics and antiferroelectrics. *International Journal of Modern Physics B* **2003**, *17*, 4355-4360, doi:10.1142/s0217979203022441.

80. Kalyani, A.K.; Senyshyn, A.; Ranjan, R. Polymorphic phase boundaries and enhanced piezoelectric response in extended composition range in the lead free ferroelectric BaTi1-xZrxO3. *Journal of Applied Physics* **2013**, *114*, doi:10.1063/1.4812472.
81. Chen, M.; Xu, Z.; Chu, R.; Liu, Y.; Shao, L.; Li, W.; Gong, S.; Li, G. Polymorphic phase transition and enhanced piezoelectric properties in (Ba0.9Ca0.1)(Ti1-xSnx)O-3 lead-free ceramics. *Materials Letters* **2013**, *97*, 86-89, doi:10.1016/j.matlet.2012.12.067.
82. Yu, Z.; Ang, C.; Guo, R.Y.; Bhalla, A.S. Piezoelectric and strain properties of Ba(Ti1-xZrx)O-3 ceramics. *Journal of Applied Physics* **2002**, *92*, 1489-1493, doi:10.1063/1.1487435.
83. Rachakom, A.; Jiansirisomboon, S.; Watcharapasorn, A. Effect of poling on piezoelectric and ferroelectric properties of Bi0.5Na0.5Ti1-xZrxO3 ceramics. *Journal of Electroceramics* **2014**, *33*, 105-110, doi:10.1007/s10832-014-9939-8.
84. Kim, J.; Loh, K.J.; Lynch, J.P. Piezoelectric polymeric thin films tuned by carbon nanotube fillers. In *Sensors and Smart Structures Technologies for Civil, Mechanical, and Aerospace Systems 2008, Pts 1 and 2*, Tomizuka, M., Ed. 2008; Vol. 6932.
85. El Achaby, M.; Arrakhiz, F.Z.; Vaudreuil, S.; Essassi, E.M.; Qaiss, A. Piezoelectric beta-polymorph formation and properties enhancement in graphene oxide - PVDF nanocomposite films. *Applied Surface Science* **2012**, *258*, 7668-7677, doi:10.1016/j.apsusc.2012.04.118.
86. Batth, A.; Mueller, A.; Rakesh, L.; Mellinger, A. Electrical properties of poly(vinylidene fluoride-hexafluoropropylene) (PVDF-HFP) blended with carbon nanotubes. In Proceedings of Electrical Insulation & Dielectric Phenomena.
87. Rahman, M.A.; Lee, B.-C.; Phan, D.-T.; Chung, G.-S. Fabrication and characterization of highly efficient flexible energy harvesters using PVDF-graphene nanocomposites. *Smart Materials and Structures* **2013**, *22*, doi:10.1088/0964-1726/22/8/085017.
88. Huang, L.; Lu, C.; Wang, F.; Wang, L. Preparation of PVDF/graphene ferroelectric composite films by in situ reduction with hydrobromic acids and their properties. *Rsc Advances* **2014**, *4*, 45220-45229, doi:10.1039/c4ra07379g.
89. Shetty, S.; Mahendran, A.; Anandhan, S. Development of a new flexible nanogenerator from electrospun nanofabric based on PVDF/talc nanosheet composites. *Soft Matter* **2020**, *16*, 5679-5688, doi:10.1039/D0SM00341G.
90. Sun, D.H.; Chang, C.; Li, S.; Lin, L.W. Near-field electrospinning. *Nano Letters* **2006**, *6*, 839-842, doi:10.1021/nl0602701.
91. Di Camillo, D.; Fasano, V.; Ruggieri, F.; Santucci, S.; Lozzi, L.; Camposeo, A.; Pisignano, D. Near-field electrospinning of light-emitting conjugated polymer nanofibers. *Nanoscale* **2013**, *5*, 11637-11642, doi:10.1039/c3nr03094f.
92. Yun, J.S.; Park, C.K.; Jeong, Y.H.; Cho, J.H.; Paik, J.-H.; Yoon, S.H.; Hwang, K.-R. The Fabrication and Characterization of Piezoelectric PZT/PVDF Electrospun Nanofiber Composites. *Nanomaterials and Nanotechnology* **2016**, *6*, doi:10.5772/62433.
93. Yun, J.S.; Park, C.K.; Cho, J.H.; Paik, J.-H.; Jeong, Y.H.; Nam, J.-H.; Hwang, K.-R. The effect of PVP contents on the fiber morphology and piezoelectric characteristics of PZT nanofibers prepared by electrospinning. *Materials Letters* **2014**, *137*, 178-181, doi:10.1016/j.matlet.2014.08.139.
94. Lee, J.S.; Shin, K.Y.; Cheong, O.J.; Kim, J.H.; Jang, J. Highly Sensitive and Multifunctional Tactile Sensor Using Free-standing ZnO/PVDF Thin Film with Graphene Electrodes for Pressure and Temperature Monitoring. *Sci Rep* **2015**, *5*, 8, doi:10.1038/srep07887.
95. Shin, K.-Y.; Lee, J.S.; Jang, J. Highly sensitive, wearable and wireless pressure sensor using free-standing ZnO nanoneedle/PVDF hybrid thin film for heart rate monitoring. *Nano Energy* **2016**, *22*, 95-104, doi:10.1016/j.nanoen.2016.02.012.
96. Xin, Y.; Qi, X.; Tian, H.; Guo, C.; Li, X.; Lin, J.; Wang, C. Full-fiber piezoelectric sensor by straight PVDF/nanoclay nanofibers. *Materials Letters* **2016**, *164*, 136-139, doi:10.1016/j.matlet.2015.09.117.
97. Hu, X.; Yan, X.; Gong, L.; Wang, F.; Xu, Y.; Feng, L.; Zhang, D.; Jiang, Y. Improved Piezoelectric Sensing Performance of P(VDF-TrFE) Nanofibers by Utilizing BTO Nanoparticles and Penetrated Electrodes. *Acs Applied Materials & Interfaces* **2019**, *11*, 7379-7386, doi:10.1021/acsami.8b19824.
98. Wu, C.M.; Chou, M.H. Polymorphism, piezoelectricity and sound absorption of electrospun PVDF membranes with and without carbon nanotubes. *Composites Science and Technology* **2016**, *127*, 127-133, doi:10.1016/j.compscitech.2016.03.001.
99. Hosseini, S.M.; Yousefi, A.A. Piezoelectric sensor based on electrospun PVDF-MWCNT-Cloisite 30B hybrid nanocomposites. *Organic Electronics* **2017**, *50*, 121-129, doi:10.1016/j.orgel.2017.07.035.

100. Lins, L.C.; Wianny, F.; Livi, S.; Dehay, C.; Duchet-Rumeau, J.; Gerard, J.-F. Effect of polyvinylidene fluoride electrospun fiber orientation on neural stem cell differentiation. *Journal of Biomedical Materials Research Part B-Applied Biomaterials* **2017**, *105*, 2376-2393, doi:10.1002/jbm.b.33778.
101. Zheng, J.; He, A.; Li, J.; Han, C.C. Polymorphism control of poly(vinylidene fluoride) through electrospinning. *Macromolecular Rapid Communications* **2007**, *28*, 2159-2162, doi:10.1002/marc.200700544.
102. Pu, J.; Yan, X.; Jiang, Y.; Chang, C.; Lin, L. Piezoelectric actuation of direct-write electrospun fibers. *Sensors and Actuators a-Physical* **2010**, *164*, 131-136, doi:10.1016/j.sna.2010.09.019.
103. Khalifa, M.; Deeksha, B.; Mahendran, A.; Anandhan, S. Synergism of Electrospinning and Nano-alumina Trihydrate on the Polymorphism, Crystallinity and Piezoelectric Performance of PVDF Nanofibers. *Jom* **2018**, *70*, 1313-1318, doi:10.1007/s11837-018-2811-6.
104. Lei, T.; Yu, L.; Wang, L.; Yang, F.; Sun, D. Predicting Polymorphism of Electrospun Polyvinylidene Fluoride Membranes by Their Morphologies. *Journal of Macromolecular Science Part B-Physics* **2015**, *54*, 91-101, doi:10.1080/00222348.2014.983853.
105. Sinha, T.K.; Ghosh, S.K.; Maiti, R.; Jana, S.; Adhikari, B.; Mandal, D.; Ray, S.K. Graphene-Silver-Induced Self-Polarized PVDF-Based Flexible Plasmonic Nanogenerator Toward the Realization for New Class of Self Powered Optical Sensor. *Acs Applied Materials & Interfaces* **2016**, *8*, 14986-14993, doi:10.1021/acsami.6b01547.
106. Jin, L.; Zheng, Y.; Liu, Z.; Li, J.; Zhai, R.; Chen, Z.; Li, Y. Design of an Ultrasensitive Flexible Bend Sensor Using a Silver-Doped Oriented Poly(vinylidene fluoride) Nanofiber Web for Respiratory Monitoring. *Acs Applied Materials & Interfaces* **2020**, *12*, 1359-1367, doi:10.1021/acsami.9b18823.
107. Das, A.; Pisana, S.; Chakraborty, B.; Piscanec, S.; Saha, S.K.; Waghmare, U.V.; Novoselov, K.S.; Krishnamurthy, H.R.; Geim, A.K.; Ferrari, A.C., et al. Monitoring dopants by Raman scattering in an electrochemically top-gated graphene transistor. *Nature Nanotechnology* **2008**, *3*, 210-215, doi:10.1038/nnano.2008.67.
108. Shi, Y.; Dong, X.; Chen, P.; Wang, J.; Li, L.-J. Effective doping of single-layer graphene from underlying SiO2 substrates. *Physical Review B* **2009**, *79*, doi:10.1103/PhysRevB.79.115402.
109. Losurdo, M.; Bergmair, I.; Dastmalchi, B.; Kim, T.-H.; Giangregroio, M.M.; Jiao, W.; Bianco, G.V.; Brown, A.S.; Hingerl, K.; Bruno, G. Graphene as an Electron Shuttle for Silver Deoxidation: Removing a Key Barrier to Plasmonics and Metamaterials for SERS in the Visible. *Advanced Functional Materials* **2014**, *24*, 1864-1878, doi:10.1002/adfm.201303135.
110. Maiti, R.; Sinha, T.K.; Mukherjee, S.; Adhikari, B.; Ray, S.K. Enhanced and Selective Photodetection Using Graphene-Stabilized Hybrid Plasmonic Silver Nanoparticles. *Plasmonics* **2016**, *11*, 1297-1304, doi:10.1007/s11468-015-0175-0.
111. Kravets, V.G.; Jalil, R.; Kim, Y.J.; Ansell, D.; Aznakayeva, D.E.; Thackray, B.; Britnell, L.; Belle, B.D.; Withers, F.; Radko, I.P., et al. Graphene-protected copper and silver plasmonics. *Sci Rep* **2014**, *4*, doi:10.1038/srep05517.
112. Gan, W.C.; Abd Majid, W.H. Effect of TiO2 on enhanced pyroelectric activity of PVDF composite. *Smart Materials and Structures* **2014**, *23*, doi:10.1088/0964-1726/23/4/045026.
113. Al-Saygh, A.; Ponnamma, D.; AlMaadeed, M.A.; Vijayan, P.P.; Karim, A.; Hassan, M.K. Flexible Pressure Sensor Based on PVDF Nanocomposites Containing Reduced Graphene Oxide- Titania Hybrid Nanolayers. *Polymers* **2017**, *9*, doi:10.3390/polym9020033.
114. Norden, A.G.W.; Lapsley, M.; Lee, P.J.; Pusey, C.D.; Scheinman, S.J.; Tam, F.W.K.; Thakker, R.V.; Unwin, R.J.; Wrong, O. Glomerular protein sieving and implications for renal failure in Fanconi syndrome. *Kidney International* **2001**, *60*, 1885-1892, doi:10.1046/j.1523-1755.2001.00016.x.
115. Mishra, M.; Roy, A.; Dash, S.; Mukherjee, S. Flexible nano-GFO/PVDF piezoelectric-polymer nano-composite films for mechanical energy harvesting. In *7th National Conference on Processing and Characterization of Materials*, Mondal, A.K., Mallik, A., Eds. 2018; Vol. 338.
116. Jaleh, B.; Jabbari, A. Evaluation of reduced graphene oxide/ZnO effect on properties of PVDF nanocomposite films. *Applied Surface Science* **2014**, *320*, 339-347, doi:10.1016/j.apsusc.2014.09.030.
117. Dodds, J.S.; Meyers, F.N.; Loh, K.J. Piezoelectric Characterization of PVDF-TrFE Thin Films Enhanced With ZnO Nanoparticles. *Ieee Sensors Journal* **2012**, *12*, 1889-1890, doi:10.1109/jsen.2011.2182043.
118. Bhunia, R.; Das, S.; Dalui, S.; Hussain, S.; Paul, R.; Bhar, R.; Pal, A.K. Flexible nano-ZnO/polyvinylidene difluoride piezoelectric composite films as energy harvester. *Applied Physics a-Materials Science & Processing* **2016**, *122*, doi:10.1007/s00339-016-0161-1.
119. Jin, C.; Hao, N.; Xu, Z.; Trase, I.; Nie, Y.; Dong, L.; Closson, A.; Chen, Z.; Zhang, J.X.J. Flexible piezoelectric nanogenerators using metal-doped ZnO-PVDF films. *Sensors and Actuators a-Physical* **2020**, *305*, doi:10.1016/j.sna.2020.111912.

120. Nuraeva, A.S.; Zelenovskiy, P.S.; Slashchev, A.; Gruzdev, D.A.; Slepukhin, P.A.; Olshevskaya, V.A.; Krasnov, V.P.; Shur, V.Y. Morphology and piezoelectric characterization of thin films and microcrystals of ortho-carboranyl derivatives of (S)-glutamine and (S)-asparagine. *Ferroelectrics* **2017**, *509*, 113-123, doi:10.1080/00150193.2017.1295430.
121. Stapleton, A.; Noor, M.R.; Sweeney, J.; Casey, V.; Kholkin, A.L.; Silien, C.; Gandhi, A.A.; Soulimane, T.; Tofail, S.A.M. The direct piezoelectric effect in the globular protein lysozyme. *Applied Physics Letters* **2017**, *111*, doi:10.1063/1.4997446.
122. Vu, N.; Zhu, R.; Jenkins, K.; Yang, R. Self-assembly of diphenylalanine peptide with controlled polarization for power generation. *Nature Communications* **2016**, *7*, doi:10.1038/ncomms13566.
123. Yang, Y.; Pan, H.; Xie, G.; Jiang, Y.; Chen, C.; Su, Y.; Wang, Y.; Tai, H. Flexible piezoelectric pressure sensor based on polydopamine-modified BaTiO3/PVDF composite film for human motion monitoring. *Sensors and Actuators a-Physical* **2020**, *301*, doi:10.1016/j.sna.2019.111789.
124. Tamang, A.; Ghosh, S.K.; Garain, S.; Alam, M.M.; Haeberle, J.; Henkel, K.; Schmeisser, D.; Mandal, D. DNA-Assisted beta-phase Nucleation and Alignment of Molecular Dipoles in PVDF Film: A Realization of Self-Poled Bioinspired Flexible Polymer Nanogenerator for Portable Electronic Devices. *Acs Applied Materials & Interfaces* **2015**, *7*, 16143-16147, doi:10.1021/acsami.5b04161.
125. Ramadan, K.S.; Sameoto, D.; Evoy, S. A review of piezoelectric polymers as functional materials for electromechanical transducers. *Smart Materials and Structures* **2014**, *23*, doi:10.1088/0964-1726/23/3/033001.
126. Chen, S.; Li, X.; Yao, K.; Tay, F.E.H.; Kumar, A.; Zeng, K. Self-polarized ferroelectric PVDF homopolymer ultra-thin films derived from Langmuir-Blodgett deposition. *Polymer* **2012**, *53*, 1404-1408, doi:10.1016/j.polymer.2012.01.058.
127. Park, C.; Ounaies, Z.; Wise, K.E.; Harrison, J.S. In situ poling and imidization of amorphous piezoelectric polyimides. *Polymer* **2004**, *45*, 5417-5425, doi:10.1016/j.polymer.2004.05.057.
128. Li, C.; Wu, P.-M.; Lee, S.; Gorton, A.; Schulz, M.J.; Ahn, C.H. Flexible dome and bump shape piezoelectric tactile sensors using PVDF-TrFE copolymer. *Journal of Microelectromechanical Systems* **2008**, *17*, 334-341, doi:10.1109/jmems.2007.911375.
129. Hong, C.-C.; Huang, S.-Y.; Shieh, J.; Chen, S.-H. Enhanced Piezoelectricity of Nanoimprinted Sub-20 nm Poly(vinylidene fluoride-trifluoroethylene) Copolymer Nanograss. *Macromolecules* **2012**, *45*, 1580-1586, doi:10.1021/ma202481t.
130. Sharma, T.; Je, S.-S.; Gill, B.; Zhang, J.X.J. Patterning piezoelectric thin film PVDF-TrFE based pressure sensor for catheter application. *Sensors and Actuators a-Physical* **2012**, *177*, 87-92, doi:10.1016/j.sna.2011.08.019.
131. Mallick, S.; Ahmad, Z.; Qadir, K.W.; Rehman, A.; Shakoor, R.A.; Touati, F.; Al-Muhtaseb, S.A. Effect of BaTiO3 on the sensing properties of PVDF composite-based capacitive humidity sensors. *Ceramics International* **2020**, *46*, 2949-2953, doi:10.1016/j.ceramint.2019.09.291.
132. Schulze, R.; Gessner, T.; Schueller, M.; Forke, R.; Billep, D.; Heinrich, M.; Sborikas, M.; Wegener, M.; Ieee. Integration of Piezoelectric Polymer Transducers into Microsystems for Sensing Applications. In *2012 International Symposium on Applications of Ferroelectrics Held Jointly with 11th Ieee Ecapd and Ieee Pfm*, 2012.
133. Huang, Z.M.; Zhang, Y.Z.; Kotaki, M.; Ramakrishna, S. A review on polymer nanofibers by electrospinning and their applications in nanocomposites. *Composites Science and Technology* **2003**, *63*, 2223-2253, doi:10.1016/s0266-3538(03)00178-7.
134. Wang, G.; Liu, T.; Sun, X.-C.; Li, P.; Xu, Y.-S.; Hua, J.-G.; Yu, Y.-H.; Li, S.-X.; Dai, Y.-Z.; Song, X.-Y., et al. Flexible pressure sensor based on PVDF nanofiber. *Sensors and Actuators a-Physical* **2018**, *280*, 319-325, doi:10.1016/j.sna.2018.07.057.
135. Singh, R.K.; Lye, S.W.; Miao, J. Measurement of impact characteristics in a string using electrospun PVDF nanofibers strain sensors. *Sensors and Actuators a-Physical* **2020**, *303*, doi:10.1016/j.sna.2020.111841.
136. Shi, K.; Sun, B.; Huang, X.; Jiang, P. Synergistic effect of graphene nanosheet and BaTiO3 nanoparticles on performance enhancement of electrospun PVDF nanofiber mat for flexible piezoelectric nanogenerators. *Nano Energy* **2018**, *52*, 153-162, doi:10.1016/j.nanoen.2018.07.053.
137. Chen, C.; Cai, F.; Zhu, Y.; Liao, L.; Qian, J.; Yuan, F.-G.; Zhang, N. 3D printing of electroactive PVDF thin films with high beta-phase content. *Smart Materials and Structures* **2019**, *28*, doi:10.1088/1361-665X/ab15b7.
138. Bodkhe, S.; Turcot, G.; Gosselin, F.P.; Therriault, D. One-Step Solvent Evaporation-Assisted 3D Printing of Piezoelectric PVDF Nanocomposite Structures. *Acs Applied Materials & Interfaces* **2017**, *9*, 20833-20842, doi:10.1021/acsami.7b04095.

139. Kim, H.; Torres, F.; Wu, Y.; Villagran, D.; Lin, Y.; Tseng, T.-L. Integrated 3D printing and corona poling process of PVDF piezoelectric films for pressure sensor application. *Smart Materials and Structures* **2017**, *26*, doi:10.1088/1361-665X/aa738e.
140. Kim, H.; Fernando, T.; Li, M.; Lin, Y.; Tseng, T.-L.B. Fabrication and characterization of 3D printed BaTiO3/PVDF nanocomposites. *Journal of Composite Materials* **2018**, *52*, 197-206, doi:10.1177/0021998317704709.
141. Shaikh, M.O.; Huang, Y.-B.; Wang, C.-C.; Chuang, C.-H. Wearable Woven Triboelectric Nanogenerator Utilizing Electrospun PVDF Nanofibers for Mechanical Energy Harvesting. *Micromachines* **2019**, *10*, doi:10.3390/mi10070438.
142. Bairagi, S.; Ali, S.W. Flexible lead-free PVDF/SM-KNN electrospun nanocomposite based piezoelectric materials: Significant enhancement of energy harvesting efficiency of the nanogenerator. *Energy* **2020**, *198*, doi:10.1016/j.energy.2020.117385.
143. Mokhtari, F.; Spinks, G.M.; Fay, C.; Cheng, Z.; Raad, R.; Xi, J.; Foroughi, J. Wearable Electronic Textiles from Nanostructured Piezoelectric Fibers. *Advanced Materials Technologies* **2020**, *5*, doi:10.1002/admt.201900900.
144. Ji, S.H.; Cho, Y.-S.; Yun, J.S. Wearable Core-Shell Piezoelectric Nanofiber Yarns for Body Movement Energy Harvesting. *Nanomaterials* **2019**, *9*, doi:10.3390/nano9040555.
145. Yee, W.A.; Kotaki, M.; Liu, Y.; Lu, X. Morphology, polymorphism behavior and molecular orientation of electrospun poly(vinylidene fluoride) fibers. *Polymer* **2007**, *48*, 512-521, doi:10.1016/j.polymer.2006.11.036.
146. D., L.X.Y.; Xia, Y.N. Electrospinning of Nanofibers: Reinventing the Wheel? *Advanced Materials* **2004**, *16*, 1151-1170, doi:10.1002/adma.200400719
147. Li, B.; Xu, C.; Zheng, J.; Xu, C. Sensitivity of Pressure Sensors Enhanced by Doping Silver Nanowires. *Sensors* **2014**, *14*, 9889-9899, doi:10.3390/s140609889.
148. Matthews, J.A.; Wnek, G.E.; Simpson, D.G.; Bowlin, G.L. Electrospinning of collagen nanofibers. *Biomacromolecules* **2002**, *3*, 232-238, doi:10.1021/bm015533u.
149. Meng, L.; Arnoult, O.; Smith, M.; Wnek, G.E. Electrospinning of in situ crosslinked collagen nanofibers. *Journal of Materials Chemistry* **2012**, *22*, 19412-19417, doi:10.1039/c2jm31618h.
150. Je, S.-S.; Sharma, T.; Lee, Y.; Gill, B.; Zhang, J.X.; Ieee. A THIN-FILM PIEZOELECTRIC PVDF-TrFE BASED IMPLANTABLE PRESSURE SENSOR USING LITHOGRAPHIC PATTERNING. In *2011 Ieee 24th International Conference on Micro Electro Mechanical Systems*, 2011; pp. 644-647.
151. Kim, H.; Torres, F.; Villagran, D.; Stewart, C.; Lin, Y.; Tseng, T.-L.B. 3D Printing of BaTiO3/PVDF Composites with Electric In Situ Poling for Pressure Sensor Applications. *Macromolecular Materials and Engineering* **2017**, *302*, doi:10.1002/mame.201700229.
152. Huang, L.; Lu, C.; Wang, F.; Dong, X. Piezoelectric property of PVDF/graphene composite films using 1H, 1H, 2H, 2H-Perfluorooctyltriethoxysilane as a modifying agent. *Journal of Alloys and Compounds* **2016**, *688*, 885-892, doi:10.1016/j.jallcom.2016.07.058.
153. Spanu, A.; Pinna, L.; Viola, F.; Seminara, L.; Valle, M.; Bonfiglio, A.; Cosseddu, P. A high-sensitivity tactile sensor based on piezoelectric polymer PVDF coupled to an ultra-low voltage organic transistor. *Organic Electronics* **2016**, *36*, 57-60, doi:10.1016/j.orgel.2016.05.034.
154. Hsu, Y.-J.; Jia, Z.; Kymissis, I. A Locally Amplified Strain Sensor Based on a Piezoelectric Polymer and Organic Field-Effect Transistors. *Ieee Transactions on Electron Devices* **2011**, *58*, 910-917, doi:10.1109/ted.2010.2102631.
155. Liu, Z.; Yang, X.; Sun, J.; Ma, F. PVDF modified Pd-SnO2 hydrogen sensor with stable response under high humidity. *Materials Letters* **2018**, *212*, 283-286, doi:10.1016/j.matlet.2017.10.105.
156. Imai, Y.; Tadaki, D.; Ma, T.; Kimura, Y.; Hirano-Iwata, A.; Niwano, M. Response characteristics of hydrogen gas sensor with porous piezoelectric poly(vinylidene fluoride) film. *Sensors and Actuators B-Chemical* **2017**, *247*, 479-489, doi:10.1016/j.snb.2017.03.001.
157. Mallick, S.; Ahmad, Z.; Touati, F.; Shakoor, R.A. Improvement of humidity sensing properties of PVDF-TiO2 nanocomposite films using acetone etching. *Sensors and Actuators B-Chemical* **2019**, *288*, 408-413, doi:10.1016/j.snb.2019.03.034.
158. Wang, G.; Xia, H.; Sun, X.-C.; Lv, C.; Li, S.-X.; Han, B.; Guo, Q.; Shi, Q.; Wang, Y.-S.; Sun, H.-B. Actuator and generator based on moisture-responsive PEDOT: PSS/PVDF composite film. *Sensors and Actuators B-Chemical* **2018**, *255*, 1415-1421, doi:10.1016/j.snb.2017.08.125.
159. Shen, H.; Ding, J.; Yuan, N.; Xu, J.; Han, L.; Zhou, X.; Fang, B. Flexible Actuator and Generator Stimulated by Organic Vapors. *Journal of Inorganic and Organometallic Polymers and Materials* **2018**, *28*, 1962-1967, doi:10.1007/s10904-018-0856-1.

160. Li, S.; Chen, S.; Zhuo, B.; Li, Q.; Liu, W.; Guo, X. Flexible Ammonia Sensor Based on PEDOT:PSS/Silver Nanowire Composite Film for Meat Freshness Monitoring. *Ieee Electron Device Letters* **2017**, *38*, 975-978, doi:10.1109/led.2017.2701879.
161. Cho, M.S.; Seo, H.J.; Nam, J.D.; Lee, Y.; Son, Y.K. A solid state actuator based on the PEDOT/NBR system: Effect of anion size of imidazolium ionic liquid. *Molecular Crystals and Liquid Crystals* **2007**, *464*, 633-638, doi:10.1080/15421400601028492.
162. Chen, K.-W.; Chen, G.-L.; Hong, C.-C. Electrodeposition of Piezoelectric Polymer Ultrasonic Transceivers for On-Chip Antibiotic Biosensors. *Journal of the Electrochemical Society* **2016**, *163*, B200-B205, doi:10.1149/2.0241606jes.
163. Lin, D.-J.; Lin, D.-T.; Young, T.-H.; Chen, T.-C.; Chang, H.-H.; Cheng, L.-P. Immobilization of DNA on Microporous PVDF Membranes by Plasma Polymerization. *Journal of Biomaterials Science-Polymer Edition* **2009**, *20*, 1943-1959, doi:10.1163/156856208x396047.
164. Zhao, B.; Hu, J.; Ren, W.; Xu, F.; Wu, X.; Shi, P.; Ye, Z.-G. A new biosensor based on PVDF film for detection of nucleic acids. *Ceramics International* **2015**, *41*, S602-S606, doi:10.1016/j.ceramint.2015.03.253.
165. Wu, Y.; Yim, J.K.; Liang, J.; Shao, Z.; Qi, M.; Zhong, J.; Luo, Z.; Yan, X.; Zhang, M.; Wang, X., et al. Insect-scale fast moving and ultrarobust soft robot. *Science Robotics* **2019**, *4*, doi:10.1126/scirobotics.aax1594.
166. Simaite, A.; Tondu, B.; Soueres, P.; Bergaud, C. Hybrid PVDF/PVDF-graft-PEGMA Membranes for Improved Interface Strength and Lifetime of PEDOT:PSS/PVDF/Ionic Liquid Actuators. *Acs Applied Materials & Interfaces* **2015**, *7*, 19966-19977, doi:10.1021/acsami.5b04578.
167. Xiao, P.; Yi, N.; Zhang, T.; Huang, Y.; Chang, H.; Yang, Y.; Zhou, Y.; Chen, Y. Construction of a Fish-like Robot Based on High Performance Graphene/PVDF Bimorph Actuation Materials. *Advanced Science* **2016**, *3*, doi:10.1002/advs.201500438.
168. Nguyen, K.T.; Ko, S.Y.; Park, J.-O.; Park, S. Miniaturized Terrestrial Walking Robot Using PVDF/PVP/PSSA Based Ionic Polymer-Metal Composite Actuator. *Journal of Mechanisms and Robotics-Transactions of the Asme* **2016**, *8*, doi:10.1115/1.4032407.